https://doi.org/10.1093/plcell/koac302 THE PLANT CELL 2023: 35: 409–434

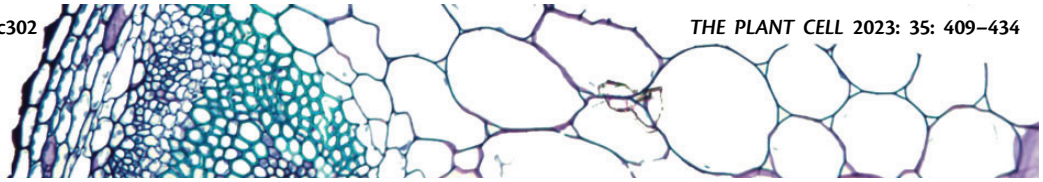

Research Article

Nitrogen-dependent binding of the transcription factor PBF1 contributes to the balance of protein and carbohydrate storage in maize endosperm

Lihua Ning ,[1] Yuancong Wang ,[1] Xi Shi ,[1] Ling Zhou ,[1] Min Ge ,[1] Shuaiqiang Liang ,[1] Yibo Wu ,[1] Tifu Zhang [1] and Han Zhao [1,*]

1 Institute of Crop Germplasm and Biotechnology, Jiangsu Provincial Key Laboratory of Agrobiology, Jiangsu Academy of Agricultural Sciences, Nanjing, Jiangsu, 210014, China

*Author for correspondence: zhaohan@jaas.ac.cn

These authors contributed equally to this work (L.N. and Y.C.W.)

L.N., H.Z., and Y.C.W. contributed to the design of the research. L.N., and X.S. performed experiments; Y.C.W., M.G., S.L., Y.B.W., and T.Z. provided technical assistance; L.N. and L.Z. analyzed data; L.N., Y.C.W. and H.Z. wrote and revised the manuscript.

The author responsible for distribution of materials integral to the findings presented in this article in accordance with the policy described in the Instructions for Authors (https://academic.oup.com/plcell/) is: Han Zhao (zhaohan@jaas.ac.cn).

Abstract

Fluctuations in nitrogen (N) availability influence protein and starch levels in maize (*Zea mays*) seeds, yet the underlying mechanism is not well understood. Here, we report that N limitation impacted the expression of many key genes in N and carbon (C) metabolism in the developing endosperm of maize. Notably, the promoter regions of those genes were enriched for P-box sequences, the binding motif of the transcription factor prolamin-box binding factor 1 (PBF1). Loss of PBF1 altered accumulation of starch and proteins in endosperm. Under different N conditions, PBF1 protein levels remained stable but PBF1 bound different sets of target genes, especially genes related to the biosynthesis and accumulation of N and C storage products. Upon N-starvation, the absence of PBF1 from the promoters of some *zein* genes coincided with their reduced expression, suggesting that PBF1 promotes zein accumulation in the endosperm. In addition, PBF1 repressed the expression of *sugary1* (*Su1*) and *starch branching enzyme 2b* (*Sbe2b*) under normal N supply, suggesting that, under N-deficiency, PBF1 redirects the flow of C skeletons for zein toward the formation of C compounds. Overall, our study demonstrates that PBF1 modulates C and N metabolism during endosperm development in an N-dependent manner.

Introduction

Maize (*Zea mays*) endosperm is a storage tissue in seeds that represents the bulk of the edible portion of maize seeds, with proteins and starch accounting for around 10% and 70%, respectively, of the total endosperm dry weight (Zhang et al., 2016). Starch is synthesized from the monosaccharides fructose and glucose, which are joined to produce the disaccharide sucrose, which is then transported into seeds (Maitz et al., 2001; Zheng, 2009; Zhang et al., 2019a). The series of enzymes involved in synthesizing starch and assembling it into semicrystalline starch granules is well characterized and includes sucrose synthase, ADP-glucose pyrophosphorylase, soluble starch synthase, granule-bound starch synthase, starch branching enzyme (SBE), and starch debranching enzyme (Hennen-Bierwagen et al., 2008; Huang et al., 2021).

Although starch is the dominant component of maize endosperm, proteins contribute considerably to the nutritional

Received June 28, 2022. Accepted October 07, 2022. Advance access publication October 12, 2022

IN A NUTSHELL

Background: Starch and protein are the main components of maize (*Zea mays*) endosperm. Nitrogen (N) fluctuation affects starch and protein levels in the endosperm. Earlier work in maize indicated that several transcription factors (TFs), such as Opaque 2, prolamin-box-binding factor 1 (PBF1), Opaque11, and ZmbZIP22 regulate the expression of genes related to starch and protein metabolism in maize endosperm. However, whether there are any TFs responsible for altering protein and starch contents in maize endosperm under limited N conditions, and the corresponding regulatory mechanisms, remain largely unknown.

Question: Are there any TFs responsible for altering starch and protein levels in maize endosperm under N deficiency conditions. If so, how does this regulation work?

Findings: We observed that N deficiency affected the expression of many key genes in N and carbon (C) metabolism in the developing endosperm of maize and that P-box motifs were enriched in the promoter regions of these key genes associated with N and C biosynthesis and metabolism. The loss of PBF1 led to altered accumulation of starch and protein in maize endosperm. Notably, even though PBF1 protein levels remained stable under different N conditions, PBF1 bound different sets of target genes, especially genes related to the biosynthesis and accumulation of N and C storage products. We also demonstrated that PBF1 repressed the expression of *Su1* and *Sbe2b* under normal N supply. We concluded that PBF1 is involved in modulating N and C metabolism during maize endosperm development in an N-dependent manner.

Next steps: To better understand the mechanisms of PBF1 in regulating the balance of protein and carbohydrate storage in an N-dependent manner, we will explore the posttranscriptional and/or translation regulation of PBF1 and identify other transcript factors that potentially interact with PBF1 to coordinate the balance of storage protein and starch components under different N conditions.

value of maize kernels. In particular, prolamins (also called zeins in maize), which are deficient in essential amino acids such as lysine and tryptophan, can make up more than 60% of the total storage proteins in maize endosperm (Wu and Messing, 2012). According to their solubility and ability to form disulfide bonds, zeins can be classified as α- (19 kD and 22 kD), β- (15 kD), γ- (50 kD, 27 kD, and 16 kD), and δ- (18 kD and 10 kD) types (Holding and Larkins, 2009). Thus, starch and protein biosynthesis in maize endosperm is a complex process involving many enzymes (Li and Song, 2020; Huang et al., 2021).

During maize reproductive growth, amino acids are transported into developing seeds and used to synthesize proteins. In particular, glutamate and glutamine are crucial for protein biosynthesis in maize as they donate NH_4^+ to all other amino acids. Glutamate is synthesized from 2-oxoglutarate (2OG) or α-ketoglutarate (Zheng, 2009), which are produced from sucrose and glucose via glycolysis and the tricarboxylic acid cycle (Zheng, 2009). Thus, the C skeletons, ATP, and reductants that are required for N metabolism can be provided by C metabolic pathways such as the tricarboxylic acid cycle and glycolysis (Sweetlove et al., 2010). Meanwhile, N-containing compounds, such as enzymes, amino acids, and nucleotides, are necessary for C metabolism (Crawford and Forde, 2002). When N levels are altered, the deposition of proteins and starch in maize kernels is greatly affected (Tsai et al., 1978; Singletary and Below, 1989; Singletary et al., 1990). When the N supply is reduced, zein accumulation is significantly reduced in maize kernels in a genotype-dependent manner (Tsai et al., 1978). By contrast, the relative starch content in endosperm increases with decreasing N supply (Singletary and Below, 1989). In addition, there is a negative relationship between starch and protein contents in endosperm from maize plants of different genotypes and grown under various N conditions (Uribelarrea et al., 2004; Triboi et al., 2006; Seebauer et al., 2010). Thus, N and C metabolism are tightly coordinated to allow proper deposition of these nutritional storage compounds in maize endosperm.

Several transcription factors (TFs) regulate the expression of genes involved in starch and protein metabolism in maize endosperm (Chen et al., 2015; Li et al., 2015; Li et al., 2018; Zhan et al., 2018; Zhang et al., 2019b). Opaque 2 (O2), a well-known endosperm-specific TF, regulates the expression of *zein* genes as well as those involved in the biosynthesis and metabolism of carbohydrates and lipids (Li et al., 2015; Zhang et al., 2016; Zhan et al., 2018; Deng et al., 2020). Prolamin-box-binding factor 1 (PBF1) is TF that belongs to an endosperm-specific protein family known as the DNA-binding one zinc finger (Dof) family. PBF1 binds to the conserved DNA sequence AAAG, a motif referred to as the P-box in cereals (Vicente-Carbajosa et al., 1997; Wang et al., 1998). It is essential for the synchronized expression of *zein* genes at 10 d after pollination (DAP; Marzábal et al., 2008; Wu and Messing, 2012). In addition, PBF1 can activate the promoters of the genes encoding pyruvate orthophosphate dikinase (PPDK) and starch synthase III (SSIII), which are important enzymes involved in starch biosynthesis. Notably, PBF1 can interact with synergistically with the TF Opaque2 (O2) to transactivate the expression of *PPDK* and *SSIII*

(Zhang et al., 2016), indicating that PBF1 is likely involved in the regulation of both C and N metabolism.

Fluctuations in N supply affect the expression of genes involved in a wide range of functions such as signal transduction, N metabolism, and molecular transport (Gutiérrez, 2012; Jiang et al., 2018). These changes alter the composition of starch and proteins in endosperm and affect nutritional value. To understand how N levels affect the deposition of starch and proteins in endosperm, we performed a transcriptome deep-sequencing (RNA-seq) analysis using the endosperm from plants grown in the presence of sufficient N (SN) or deficient N (DN). We found that the P-box sequence is enriched in the promoters of differentially expressed genes (DEGs) in SN vs. DN conditions, suggesting that PBF1 modulates the expression of DEGs that regulate the levels of C and N compounds in endosperm. We also observed that PBF1 altered the accumulation of starch and proteins in endosperm under DN conditions. A combination of chromatin immunoprecipitation followed by sequencing (ChIP-seq) and RNA-seq analyses showed that the binding pattern of PBF1, rather than its abundance, was altered based on N availability. These results suggest that PBF1 contributes to C and N assimilation in developing endosperm from plants grown under different N conditions through an N-dependent mechanism.

Results

N deficiency causes elevated carbohydrate levels and depletion of storage proteins in maize endosperm

To evaluate the effects of N supply on the maize kernels, we harvested the seeds of maize plants (B73) grown under DN or SN conditions. Samples were collected from developing endosperm at 15 days after pollination (DAP) and mature endosperm at 40 DAP. The 100-kernel weight (g/100 seeds) of mature dry seeds grown under DN conditions was reduced by 24.1% compared with seeds grown under SN conditions (Figure 1A). Upon N limitation, we observed reductions in the total protein content (38.4% reduction in developing endosperm and 17.8% in mature endosperm) and zein content (39.4% reduction in developing endosperm and 29.2% mature endosperm limitation (Figure 1, B and C). In contrast to the protein content, starch content was increased both in developing endosperm (26.9% increase) and in mature endosperm (18.7% increase) from plants grown under DN conditions compared with those grown under SN conditions (Figure 1D). Concentrations of soluble sugars and total free amino acids were also altered by N limitation (Figure 1, E and F). These results suggested that N limitation has distinct impacts on the accumulation of proteins and carbohydrates in maize endosperm, leading to altered ratios of these compounds in seeds.

The expression of genes involved in C and N metabolisms is influenced by N limitation

We examined the expression levels of key genes involved in starch biosynthesis at different stages of endosperm development. As shown in Supplemental Figure S1, most of the genes related to C and N biosynthesis and metabolism, such as *PPDKs*, *AGPS1a* (which encodes the small subunit of AGP1), *Su1*, and *Pho1*, were expressed at higher levels at 15 DAP than at 24 DAP. Moreover, a previous study indicated that the majority of the zein-related genes reached their maximum expression levels at 14 DAP and stayed stable till 30 DAP (Chen et al., 2014). As a result, we considered that 15 DAP was a critical stage for endosperm to initialize the accumulation of carbohydrates as well as storage proteins. For this reason, most of our subsequent analyses were focused on this stage.

To identify genes whose transcript abundance changed in response to N deficiency, we performed an RNA-seq analysis using total RNA extracted from the developing endosperm. We obtained approximately 47 million paired-end reads from each sample. Uniquely aligned reads accounted for about 79.1% of the sequenced raw reads. These reads were used to estimate the normalized transcription levels as the expected number of transcripts per million base pairs sequenced (TPM). Under DN conditions vs. SN conditions in developing endosperm, we found 4,899 differentially expressed genes (DEGs), including 1,145 downregulated and 3,754 upregulated genes (Supplemental Data Set S1). We then performed gene ontology (GO) and Kyoto encyclopedia of genes and genomes (KEGG) enrichment analyses on the above DEGs using the databases g:Profile (Uku et al., 2019) and agriGO (Tian et al., 2017), complemented by the MapMan database (Usadel et al., 2005; Supplemental Figure S2 and Supplemental Data Set S2). Based on the annotation, it appears that cellular N and carbohydrate biosynthesis/metabolism is significantly influenced by N supply (Figure 1G). The modules for C metabolism and biosynthesis of amino acids were also significantly enriched (Figure 1G). The most significantly enriched GO term related to molecular function was nutrient reservoir activity, including 16 *19-kD α-zein* genes, 11 *22-kD α-zein* genes, the *18-kD δ-zein* gene, and the *50-kD γ-zein* gene. In addition, biosynthesis of amino acids; glycine, serine, and threonine metabolism; and protein processing in endoplasmic reticulum were significantly enriched (Figure 1G). Likewise, genes related to the C metabolism were enriched among the DEGs, including those related to starch and sucrose metabolism; glycolysis/gluconeogenesis; carbon metabolism; and pyruvate metabolism (Figure 1G), with 58 genes associated with these GO terms (Figure 1G and Supplemental Data Set S2). We conclude that N deficiency predominantly altered the expression of genes related to C and N metabolism in the developing endosperm.

P-boxes are enriched in the promoter regions of the DEGs associated with C and N biosynthesis/metabolism

To screen for common *cis*-elements in the promoter regions of DEGs associated with C and N biosynthesis/metabolism (from the significantly enriched GO terms and clusters of MapMan), we retrieved the sequences between 0.5 kb

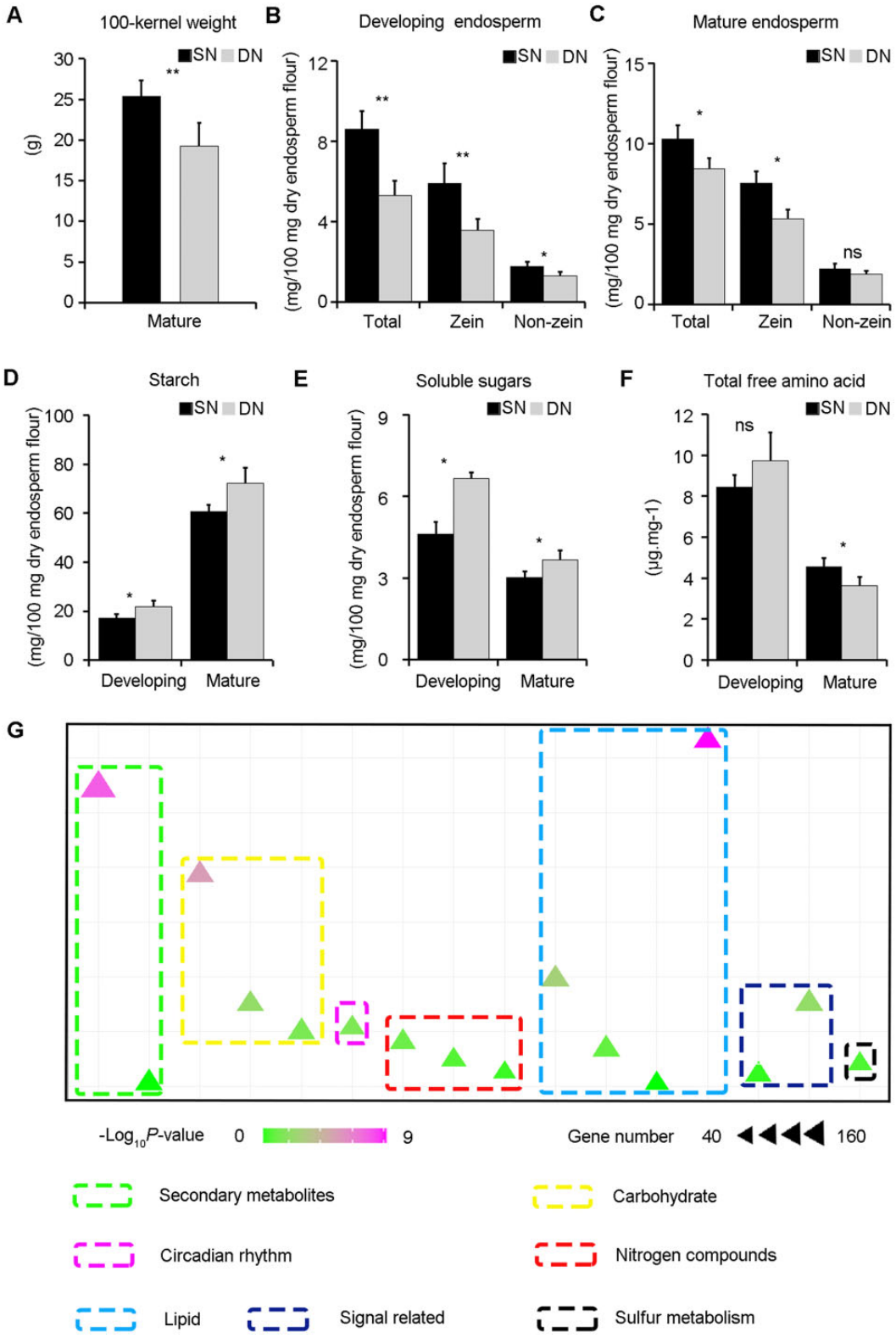

Figure 1 Storage carbohydrates and proteins in the endosperm of maize plants (B73) grown under DN and SN conditions. A, Seed weight (g/100 kernels) from plants grown under DN or SN conditions. B and C, Protein contents in B73 developing and mature endosperm grown under DN or SN conditions. D, Starch contents in B73 developing and mature endosperm grown under DN or SN conditions. E, Contents of soluble sugars in B73 developing and mature endosperm grown under DN or SN conditions. F, Concentrations of total free amino acids in B73 endosperm collected grown under DN or SN conditions. G, Enrichment analysis of DEGs (DN vs. SN) in 15 DAP endosperm grown under DN or SN conditions. Data are shown as means ± SD of three biological replicates from three different ears. Significant differences were determined using Student's *t* test. $^{*}P < 0.05$, $^{**}P < 0.01$; ns represents insignificant (Supplemental Data Set S13).

upstream of transcription start sites (TSSs) of these DEGs and performed motif enrichment analyses (Supplemental Data Sets S3 and S4). Using MEME software (Bailey et al., 2009), nine *cis*-regulatory motifs were enriched (Supplemental Figure S3 and Supplemental Table S3). To identify TFs that target these motifs, we compared the motifs to a database of known TF-binding motifs using the Tomtom (https://meme-suite.org/meme/tools/tomtom), Stamp (http://www.benoslab.pitt.edu/stamp/), and PlantCistromeDB (http://neomorph.salk.edu/PlantCistromeDB) online tools. The top four significantly enriched motifs are shown in Supplemental Figure S3.

The most significantly enriched motif (Motif 1) matched a sequence recognized by AtOBP3 and AtZNFf348, two TFs in Arabidopsis (*Arabidopsis thaliana*). In maize, ZmDOF27 and ZmDOF33 are the maize homologs of AtOBP3. However, according to our RNA-seq analysis, neither of the genes encoding these two proteins was expressed in the developing endosperm. In addition, the maize genome does not encode a homolog of AtZNFf348. The ETHYLENE-RESPONSE FACTOR (ERF) family member At4g18450, encoding a protein with an APETALA 2 (AP2) domain, recognizes the second most enriched motif in Arabidopsis. The gene encoding Ethylene-responsive element binding protein 165 (*EREB165*, Zm00001d026191), which is homologous to At4g18450, is highly expressed in root tissues (Walley et al., 2016), but was only moderately expressed in the developing endosperm in our RNA-seq analysis (SN-TPM = 12.0, DN-TPM = 12.1). The third most enriched motif contained the core sequence AAAG, which is quite similar to the P-box sequence recognized by Dof family TFs in Arabidopsis. In maize, *Pbf1* and *ZmDOF36* are specifically expressed in endosperm (Qi et al., 2017; Wu et al., 2019). Moreover, PBF1 is directly involved in C and N synthesis and metabolism in endosperm (Li et al., 2015; Zhang et al., 2016). Therefore, we hypothesized that *Pbf1* plays a regulatory role of in maize endosperm in response to different N levels.

Compromised response to N supply upon loss of PBF1

To explore the regulatory function of PBF1, we generated knockout mutants using the CRISPR-Cas9 system in the genetic background of KN5585, due to its feasibility for transformation. The guide RNA target was designed based on the sequence of the second exon of *Pbf1* (Figure 2A). One mutant, *pbf1-1* contains a four-nucleotide ACTT deletion at 254–257 bp of the *Pbf1* coding region, and a second mutant (*pbf1-2*) contains a single-nucleotide insertion of T after the 253rd bp of the *Pbf1* coding region (Figure 2B). Both events likely caused loss of PBF1 function due to a frameshift and the introduction of a premature translation termination codon. Using a specific anti-PBF1 antibody, we assessed the abundance of PBF1 in immature kernels from the *pbf1-1* and *pbf1-2* mutants at 15 DAP. No signal was detected from *pbf1-1* and *pbf1-2* kernels (Figure 2E and Supplemental Figure S4B).

Mature *pbf1* mutant kernels were smaller than wild-type (WT, a KN5585 inbred line) kernels and had an opaque phenotype (Figures 2, C and D and Supplemental Figure S4A). The 100-kernel weight in *pbf1* mutants was slightly reduced (5.8% and 7.8% in *pbf1-1* and *pbf1-2*, respectively) than that from WT plants under SN conditions (Figure 2H and Supplemental Figure S5A). We also extracted zein proteins from mature kernels of the WT and *pbf1* mutants and analyzed them using SDS-PAGE (Figure 2F). The level of all zein proteins, including 50-kD γ-zein, 27-kD γ-zein, 22-kD α-zein, and 19-kD α-zein was reduced in mutant kernels compared with that in WT (Figure 2F).

We measured the starch and protein contents in mature endosperm collected from seeds of WT and *pbf1* mutant plants grown under SN and DN conditions. Based on the genotype and the growth conditions, we divided the endosperms into four types: (1) WT endosperm grown under SN conditions (SN-WT); (2) WT endosperm grown under DN conditions (DN-WT); (3) *pbf1* mutant endosperm grown under SN conditions (SN-*pbf1*); 4. *pbf1* mutant endosperm grown under DN conditions (DN-*pbf1*). Compared with that of SN-WT, the 100-kernel weight of SN-*pbf1* was significantly reduced under SN, but the difference between WT and *pbf1* was not significant under DN conditions (Supplemental Figure S5A). Consistent with the results obtained by SDS-PAGE (Figure 2F), loss of PBF1 function led to reduced level of zein as well as total storage proteins (as measured using a BCA Protein Assay Kit); yet the impact was more significant under SN conditions (Supplemental Figure S5D). This was accompanied by increased accumulation of free amino acids in the kernels from *pbf1*, suggesting that PBF1 promotes zein biosynthesis. Starch content was elevated in *pbf1* mutants under SN conditions, but the difference was not statistically significant compared with that from WT plants (Supplemental Figure S5B). It should be noted that if the difference between WT and *pbf1* under SN conditions was compared, starch content was 1.8% and 2.3% higher in *pbf1-1* and *pbf1-2* plants than that in WT plants (57.1%, 57.6% vs. 55.3%), respectively, whereas protein content was 1.59% and 1.80% lower in *pbf1-1* and *pbf1-2* (9.7%, 9.5% vs. 11.3%, Supplemental Figure S5). As a result, the net change of starch and proteins was comparable in *pbf1* mutants. In other words, the starch content in *pbf1* was increased considerably under SN; nonetheless, the statistically significant of such increase was masked by the overall high percentage of starch in the kernel.

When the variation (Δ in Figure 2) of each component of the endosperm between SN and DN was compared, the difference for all components between the two N levels became less dramatic in *pbf1* compared with that of WT (Figure 2, G–K). The only exception was for the non-zein proteins, which demonstrated more pronounced variation between SN and DN. The reduced degree of variation of proteins and carbohydrates between SN and DN suggests

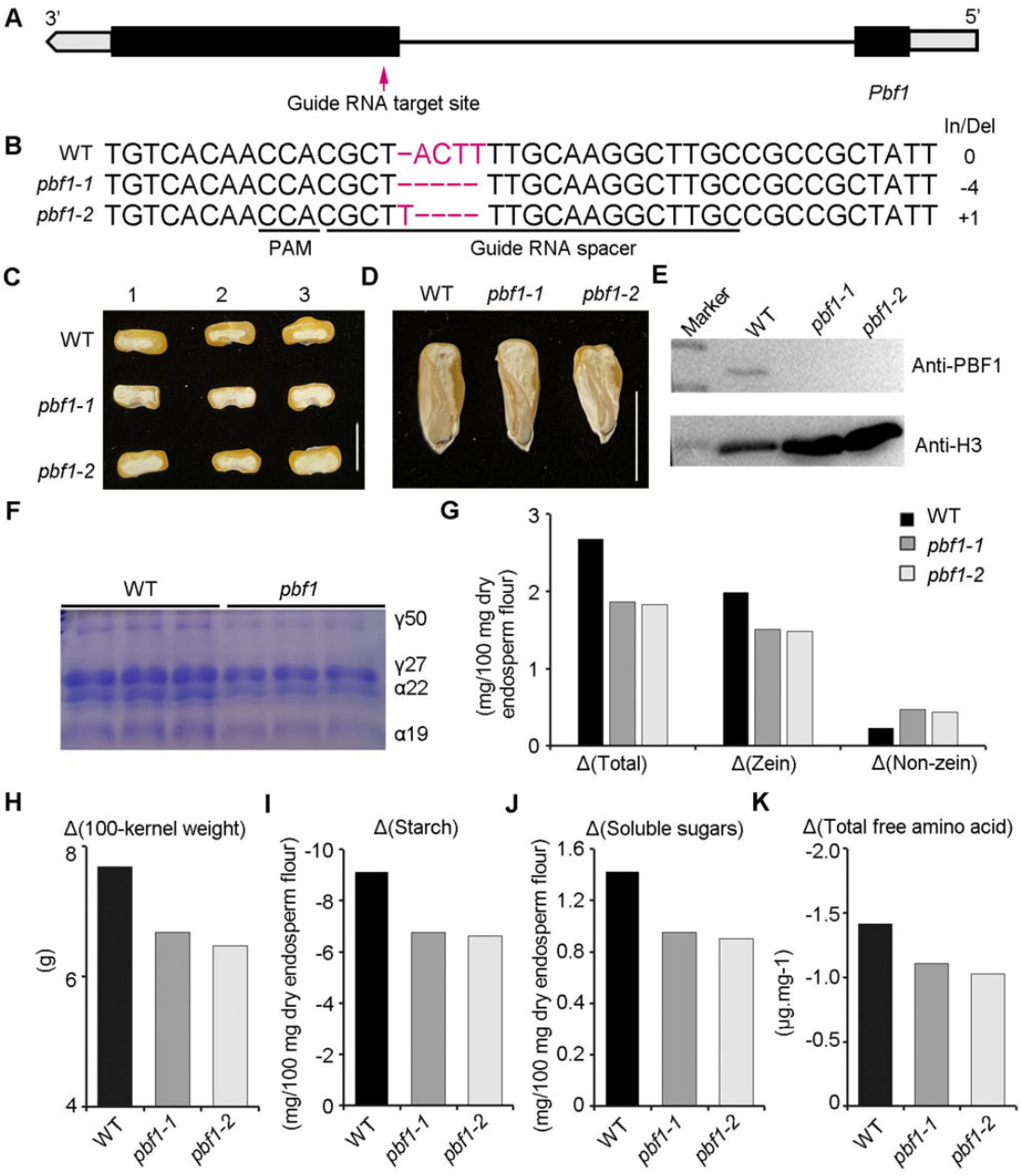

Figure 2 Phenotypes and storage-reserve contents of WT and *pbf1* endosperm. A, Schematic representation of the gene model of PBF1. The arrow indicates the guide RNA target site. B, The CRISPR/Cas9-edited sequences in *pbf1* alleles. *Pbf1-1* has a four-nucleotide ACTT deletion at 254–257 bp of the *Pbf1* coding sequence; *pbf1-2* has a single-nucleotide insertion of T after the 253th bp in the *Pbf1* coding sequence. The guide RNA spacer and the protospacer adjacent motif (PAM) site are indicates. C and D, Transverse and sagittal sections of WT (a KN5585 inbred line) and *pbf1* mature kernels. Bar = 1 cm. E, Immunoblot analysis of PBF1 showing the absence of PBF1 in *pbf1-1* and *pbf1-2*. An anti-histone H3 antibody was used as the internal control. Total proteins were extracted from whole kernels at 15 DAP. F, SDS-PAGE analysis of zein proteins in WT and *pbf1* seeds. The size of each zein protein band is indicated to the right of the image. γ50, 50-kD γ-zein; γ27, 27-kD γ-zein; α22, 22-kD α-zein; α19, 19-kD α-zein. G–K, Variation of the contents of proteins, starch, soluble sugars, total free amino acid in endosperm between plants grown under SN or DN conditions for both WT and *pbf1* mutants. The variation is the average value contents in endosperm under SN conditions minus the average value contents in endosperm under DN conditions. H, The variation of 100-kernel weight of WT (a KN5585 inbred line) and *pbf1* seeds between that grown under SN and DN conditions. The variation was defined the same way as described in (G).

that loss of PBF1 hinders plant responses to the variation of N levels. Particularly, it appears that the mutants cannot fully utilize N to produce zein proteins and achieve maximum yield potential under normal N conditions (Figure 2 and Supplemental Figure S5).

Many of the PBF1-regulated genes are involved in C and N metabolism and responsive to N limitation

To further explore the potential regulatory function of PBF1 during maize endosperm development, we performed an RNA-seq analysis of 15 DAP-developing endosperm from

pbf1 mutants and WT plants grown under SN conditions. Because the phenotypes of the two mutants were highly similar, we used *pbf1-1* as a representative to study the function of PBF1 in subsequent experiments. We considered that the DEGs between WT and *pbf1* mutants represented PBF1-regulated genes. Among the tested genes, 1,397 were detected as DEGs, including 574 that were downregulated and 823 that were upregulated in the *pbf1* mutants (Figure 3A, Supplemental Table S2, Supplemental Data Sets S5 and S6). We compared the PBF1-regulated genes identified in *pbf1* mutants to the DEGs identified in *pbf1RNAi* plants relative to WT (Zhang et al., 2016) and found that 356 DEGs from our study were also identified as DEGs in *pbf1RNAi* plants (Supplemental Figure S6), including several the key DEGs revealed by characterization of *pbf1RNAi* plants. The *PPDK1/2* transcript levels were only slightly altered in *pbf1RNAi* plants, although they were directly modulated by PBF1 (Zhang et al., 2016).

In our study, The *PPDK1/2* transcript levels were consistent with those from *pbf1RNAi* plants. The transcript level of *27-kD γ-zein* was significantly reduced in *pbf1RNAi* plants (Zhang et al., 2016), although it did not seem to be significantly altered by the complete loss of function of PBF1 at 15 DAP in our study. As mentioned above, most of the zein genes had achieved maximum expression levels at 14 DAP, yet *27-kD γ-zein* is an exception in that its expression level continued to increase after 14 DAP till 24 DAP (Chen et al., 2014).

To further understand the impact of PBF1 on expression of *27-kD γ-zein*, we conducted RT-qPCR using RNAs from the endosperm at 18 DAP and 24 DAP. As shown in Supplemental Figure S7, the expression level of *27-kD γ-zein* was significantly lower in *pbf1* compared to that in WT plants at both 18 DAP and 24 DAP, suggesting that PBF1 positively regulates the expression of *27-kD γ-zein*. Based on the annotation, genes related to cellular N and carbohydrate biosynthesis/metabolism were significantly regulated by PBF1 (Figure 3B).

We integrated the two RNA-seq data sets (*pbf1* vs WT and DN-B73 vs. SN-B73) in this study and established that the expression levels of 478 PBF1-regulated genes were altered in B73 endosperm grown under DN vs. SN conditions (Figure 3C and Supplemental Data Set S7). The overlapping DEGs were significantly enriched in "nutrient reservoir activity," including 14 zein genes. The abundance of all of the *zein* transcripts was dramatically decreased in DN-B73 endosperm compared with that in SN B73 endosperm (Figure 3D and Supplemental Data Set S7). In addition, genes in the "energy reserve metabolic process" were enriched among overlapping DEGs (Supplemental Data Set S7), including the starch synthesis genes, such as *Sbe1*, *Sbe2a*, *Sbe2b*, *Pho1*, *Su1*, and *Su4* (Supplemental Data Set S7). We then performed RT-qPCR to analyze the expression of the PBF1-regulated starch biosynthesis genes using SN-WT (KN5585) and DN-WT(KN5585) endosperm. Consistent with the transcriptome analysis, the RT-qPCR analyses confirmed that the transcript levels of starch biosynthesis genes were dramatically increased in DN-WT endosperm compared with SN-WT (Figure 3F). These results suggested that the transcript levels of PBF1-regulated genes that are involved in C and N biological processes were also altered by N limitation.

Pbf1 expression does not respond to N starvation

Because the expression of many PBF1-regulated genes was altered by N deficiency, we tested whether the expression of *Pbf1* was influenced by N levels. However, no dramatic variation in the abundance of *Pbf1* transcripts was observed between the B73 endosperm grown from plants under SN conditions (TPM = 13.6) and that grown under DN conditions (DN-TPM = 16.3). Likewise, RT-qPCR detected similar transcript levels of *Pbf1* in B73 grown under SN and DN conditions (Figure 4A). We extracted total proteins from endosperm of B73 and KN5585 plants grown under SN and DN conditions at 15 DAP and performed immunoblot assays. Consistent with the transcript levels, the PBF1 protein level showed little variation between SN and DN conditions (Figure 4, A and B and Supplemental Figure S8).

To identify whether the spatial expression of *Pbf1* was altered by N limitation, we conducted an RNA in situ hybridization assay using the 15-DAP seeds from plants grown under SN and DN conditions. *Pbf1* mRNA was mainly detected in the starchy endosperm cell, and the pattern in the developing endosperm was similar under the different N conditions (Figure 4C). Taken together, these findings indicate that N starvation has little effect on the transcription, translation, or spatial expression pattern of *Pbf1*.

Nitrogen-dependent binding of PBF1 to target genes

Because the stable expression of *Pbf1* failed to explain the enrichment of the PBF1-binding motif among DEGs between different N conditions, we hypothesized that the binding of PBF1 to its targets was affected by N availability. To test this, we performed ChIP-seq analysis using the anti-PBF1 antibody and chromatin samples extracted from endosperm of WT and *pbf1* plants grown under SN and DN conditions at 15 DAP. As a negative control, chromatin from *pbf1* mutants grown in SN and DN conditions was extracted and used for ChIP-seq assays. As shown in Supplemental Figure S9, the specific PBF1 antibody recognizes the native form of PBF1, thus meeting the requirements for a conclusive ChIP assay.

After sequencing the ChIP-seq libraries, we merged the reads mapped from each biological replicates. Significant binding peaks from the ChIP-seq analysis were defined by comparing the parallel WT and *pbf1* samples using MACS2.0 (Zhang et al., 2008). We identified 13,977 peaks in the SN endosperm and 12,132 peaks in the DN endosperm ($P < 0.001$). Genic regions were defined as the regions between 2 kb upstream of the transcription start site (TSS) and 2 kb downstream of the transcription termination site (TTS) of each coding sequence. The fraction of peaks located in genic regions in the SN endosperm (48.5%) was

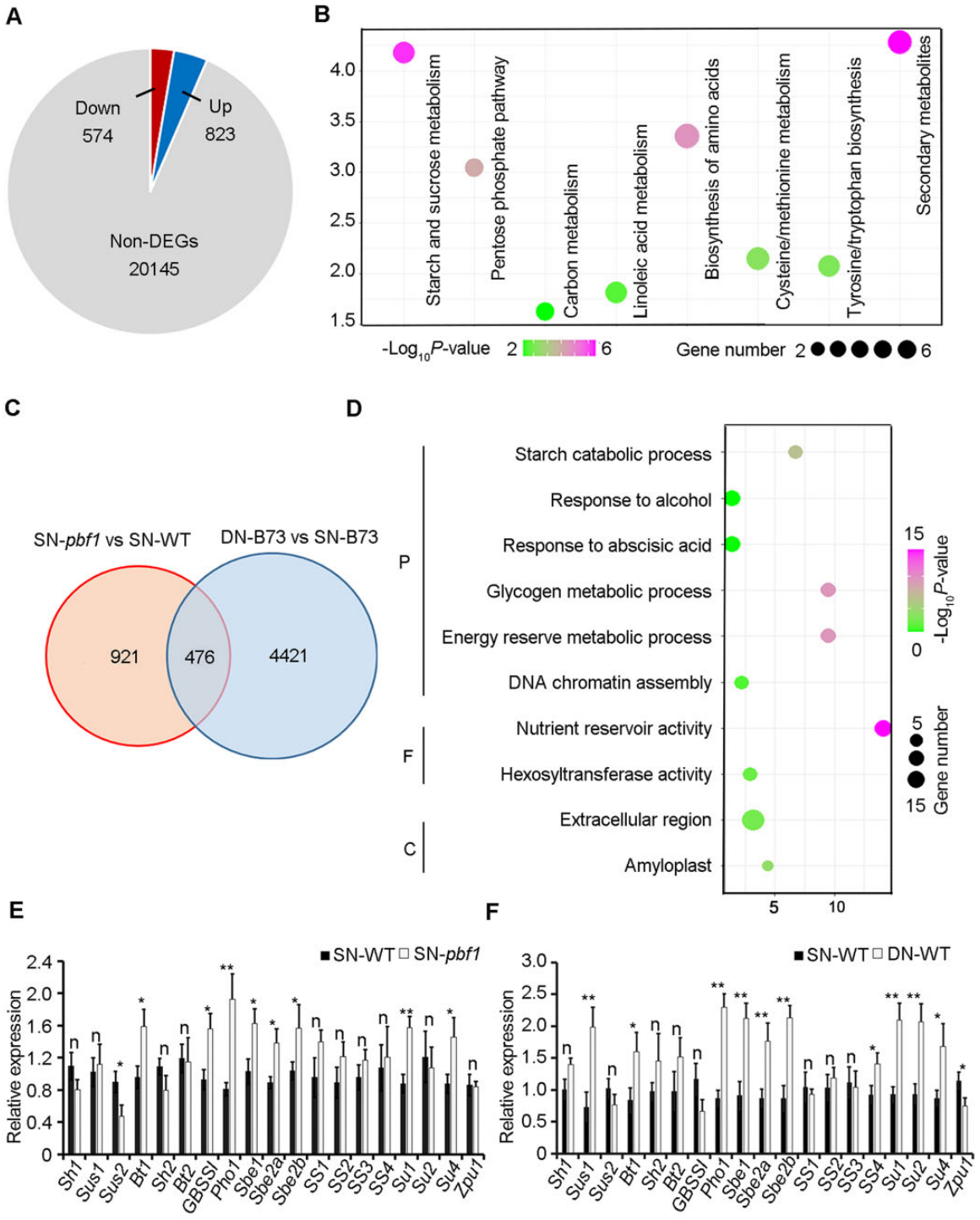

Figure 3 Comparison of transcriptomes between WT and *pbf1* endosperms. A, Pie chart showing numbers of DEGs in WT vs. *pbf1* endosperms. B, Enrichment analysis of DEGs in WT and *pbf1* endosperms. C, Venn diagram showing the overlap between DEGs regulated by PBF1 and DEGs influenced by N limitation in B73. D, Enrichment analysis of N regulated genes that were also regulated by PBF1. E and F, RT-qPCR analysis of starch biosynthetic genes in WT and *pbf1* endosperm. All expression levels were normalized to that of *ZmUPF1* (Zm00001d006438). Data are shown as means ± SD of three biological replicates from three different ears. Significant differences were determined using Student's *t* test. $^{*}P < 0.05$; $^{**}P < 0.01$, "n" represents insignificant or $|\text{Log}_2\text{fold change}| < 0.50$ (Supplemental Data Set S13).

about 1.7-fold higher than that in the DN endosperm (28.7%; Figure 5, B and C).

To assess the degree of enrichment for PBF1-binding sites in different genomic regions, we calculated the ratio of binding peaks in each region to the entire genome fraction of the corresponding region. A value >1 indicates enrichment of binding sites in that region whereas a value <1 indicates relative depletion of binding sites. In SN endosperm, the binding sites

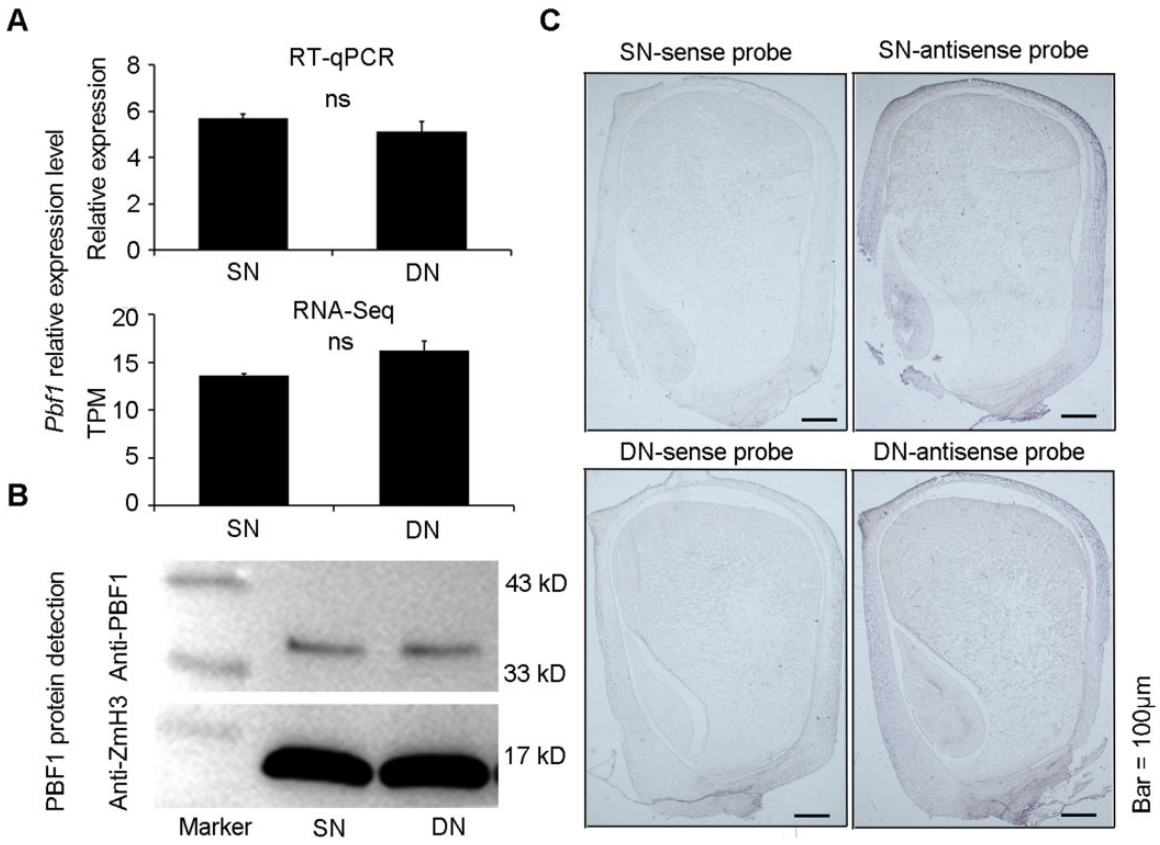

Figure 4 The expression of PBF1 in B73 developing endosperm under SN and DN conditions. A, Transcriptional levels were measured by RT-qPCR, the values were normalized using housekeeping gene *ZmUPF1* (Zm00001d006438) used as the reference gene. TPM indicates the value of TPM (transcripts per million base pairs sequenced) form RNA-seq. Data are shown as means ± SD of three biological replicates from three different ears. Significant differences were determined using Student's *t* test. ns represents insignificant (Supplemental Data Set S13). B, PBF1 protein levels as measured by immunoblot assay, using anti-H3 as a sample loading control. C, RNA in situ hybridization of *Pbf1* in developing seeds under SN conditions and DN conditions. Longitudinal sections of B73 kernels at 15 DAP were hybridized with an antisense RNA probe corresponding to *Pbf1*. The positive signals of *Pbf1* were mainly observed in the peripheral area of starchy endosperm. No signal was seen in the two sections hybridized with sense probes of *Pbf1*. Bar = 100 μm.

for PBF1 were enriched in all genic regions and were depleted in intergenic regions (Figure 5, A and D). In particular, the PBF1-binding sites in SN endosperm were enriched more than 5-fold in upstream sequences and 5′-untranslated regions (UTRs), where most *cis*-regulatory elements of genes are located. By contrast, the PBF1-binding sites in DN endosperm were only moderately enriched in flanking regions and 5′-UTRs, and were not dramatically depleted in intergenic regions (Figure 5D), suggesting a more even distribution across the genome compared with that in SN endosperm.

To test whether PBF1-binding sites were indeed adjacent to the TSSs, we profiled their distribution density by counting the number of peaks per 100-bp bins within 20 kb upstream of TSSs and 20 kb downstream of TSSs. We found that the SN peaks were skewed towards regions near the TSSs (500 bp downstream and upstream of the TSSs regions for DEGs) under SN conditions. In contrast, DN peaks were not as concentrated around TSSs as SN peaks (Figure 5E and Supplemental Figure S10), suggesting an overall reduced affinity of PBF1 for genes in developing endosperm grown under DN conditions.

We considered the genes with the binding peaks located in the regions between 2 kb upstream of TSSs as PBF1-bound target genes. A total of 2,932 and 1,445 PBF1-bound genes were identified in SN and DN endosperm, respectively (Figure 5F and Supplemental Data Set S8). Of these, only 554 PBF1 targets were common to developing endosperm grown under SN and DN conditions (Figure 5F and Supplemental Figure S11, A and B), suggesting that the binding of PBF1 to its cognate *cis*-regulatory motifs is largely dependent on the N availability. Moreover, nearly 80% of the PBF1 target genes under SN conditions were no longer associated with PBF1 upon N starvation.

We then looked for overlap between the PBF1-bound genes and the PBF1-regulated genes and found that, under SN conditions, 183 PBF1-bound and -modulated genes (here referred to as SN-PBF1 direct targets) were affected by PBF1 binding (53 were activated and 130 were repressed by PBF1). Under DN conditions, we found 109 PBF1-bound and -modulated genes (here referred to as DN-PBF1 direct targets), 21 of which were activated, and 88 were repressed by PBF1 (Figure 5F and Supplemental

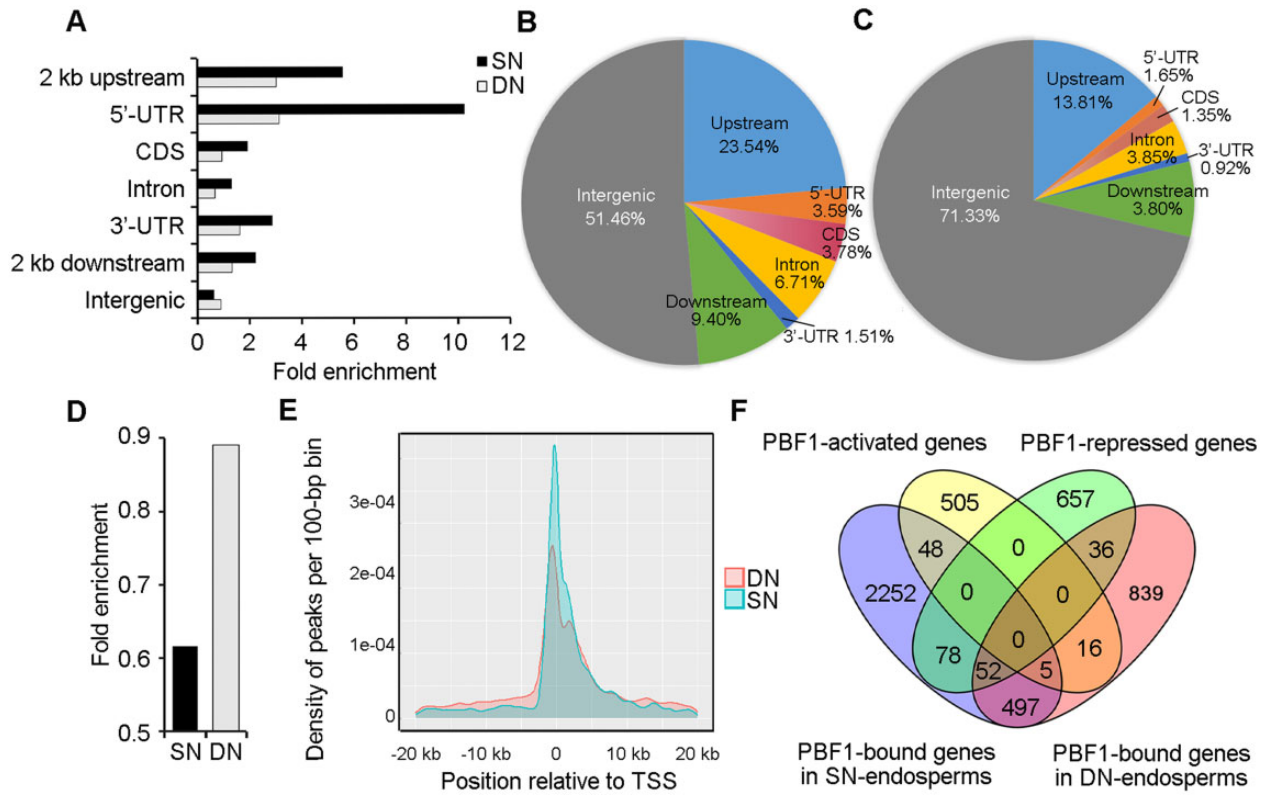

Figure 5 Identification of PBF1 target genes using ChIP-seq. A and D, The fold enrichment of PBF1 peaks in the maize genome based on the localization of peak summits under SN and DN conditions compared with the fraction of genome, respectively. B and C, Distribution of PBF1 peaks in the maize genome based on the localization of peak summits under SN (B) and DN (C) conditions, respectively. D, The fold enrichment of PBF1 peaks located intergenic under SN and DN conditions compared with the fraction of genome, respectively. Enlarged from (A) to allow visibility. The data of figure (D) was from (A). E, Frequency distributions of peaks per 100-bp bin corresponding to the distance of peaks to TSSs (transcription start sites) ranging from −20 kb to 20 kb. TSSs indicates the transcription start sites. F, Venn diagram showing the overlaps of the DEGs detected in this study and the PBF1 target genes identified by ChIP-seq.

Data Set S9). Of these, 57 common PBF1 targets (common-PBF1-direct-targets) were shared by the developing endosperm grown under SN and DN conditions. Thus, 126 (SN-specific-PBF1-direct-targets) and 52 (DN-specific-PBF1-direct-targets) were specifically bound and modulated by PBF1 under SN and DN conditions, respectively.

To identify *cis*-regulatory sequence(s) recognized by PBF1, we performed a de novo motif screening on the PBF1-binding elements that were enriched within a 401-bp region (centered at the summits of each of the peaks) for the direct PBF1 target genes under SN and DN conditions using the MEME-ChIP program. Four motifs (*E*-value < 0.05, Supplemental Table S4) were identified from the promoter regions of PBF1-bound target genes in the SN endosperm. Two of these motifs (Motif 3 and 4) contained the sequence AAAG, a core sequence of the previously described prolamin box (Figure 6, A and C). The two motifs were shown to be centrally enriched in the analyzed genomic regions ($P < 0.05$; Figure 6, B and D and Supplemental Table S4). Using the same criteria, no centrally enriched motif was detected in the analyzed genomic regions from the ChIP-seq data using the DN-endosperm, a result consistent with the low abundance of P-box-binding sites near the TSSs of genes in the DN-endosperm (Figure 5, A and F) To determine whether the P-box was bound by PBF1, an electrophoretic mobility shift assay (EMSA) was performed using eight biotin-labeled probes derived from the promoter regions of potential PBF1 targets (*Su1*, *Pho1*, *Bt1*, *Sbe2b*, *WHITE-CORE RATE 1* (*ZmWCR1*), Zm00001d053816, Zm00001d014258, and Zm00001d037576; Figure 6, E and F and Supplemental Figure S12). The in vitro binding assay indicated a strong affinity of PBF1 for each of the target probes, and the binding activity was partially abolished by the addition of cold competitor probes containing a PBF1-binding sequence (Figure 6, E and F, Supplemental Figure S12, and Supplemental Table S5). Furthermore, a subset of binding sites containing binding motifs was also tested for enrichment by ChIP-qPCR, confirming the association between PBF1 and the identified genomic regions under SN conditions (Supplemental Figures S13 and S14 and Supplemental Table S5).

Genes bound by PBF1 are involved in C and N metabolism in a nitrogen-dependent manner

Overlay of the identified SN-specific-PBF1-direct-targets (126) with the DEGs regulated by N levels indicated that the

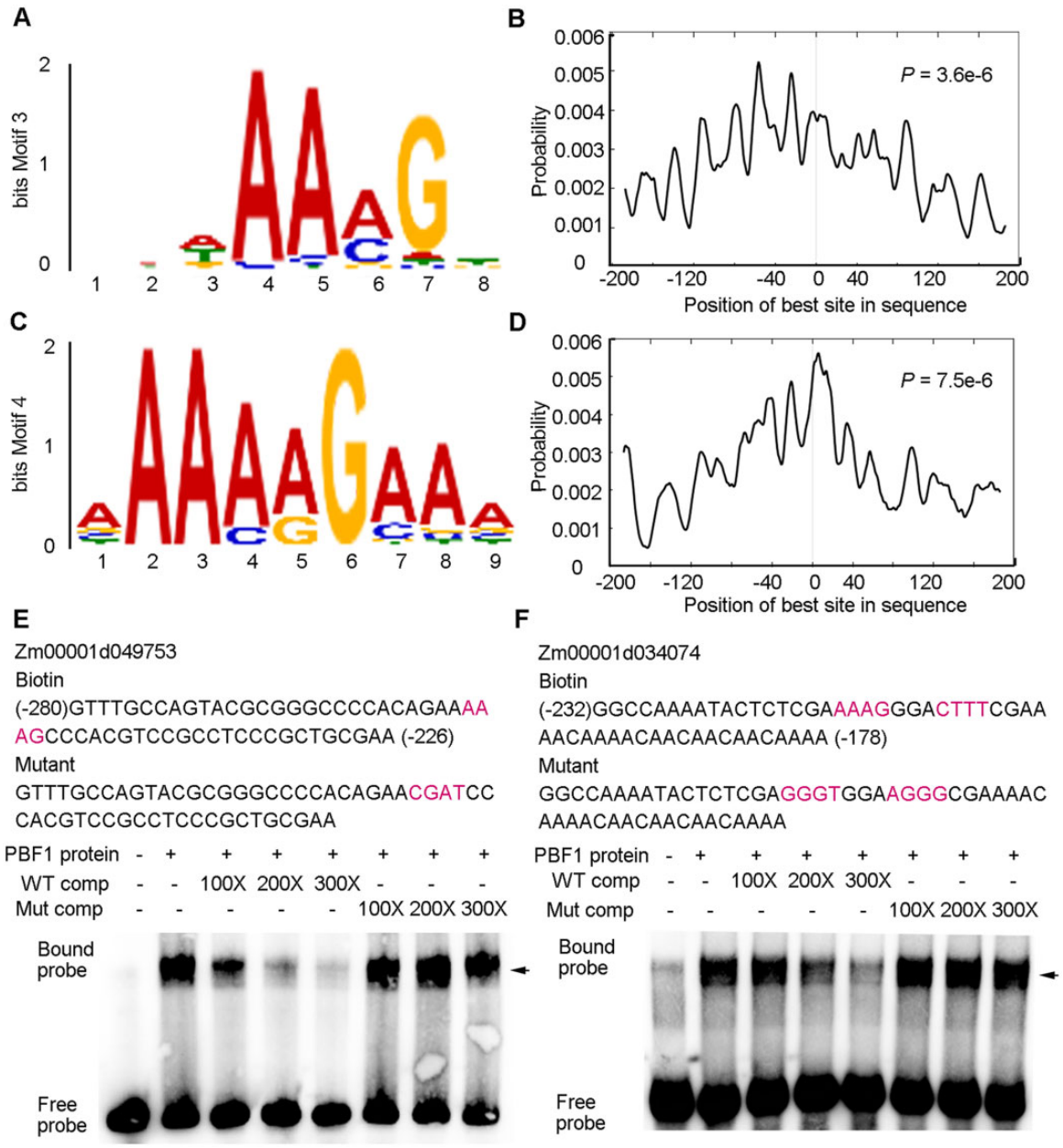

Figure 6 Sequence motifs enriched in the promoter regions of SN-PBF1-direct target genes. A and C, A P-box-like motifs and their positional distributions (B) and (D) flanking the summits of the peaks associated with PBF1-direct target genes identified in the endosperm collected from plants grown under SN conditions. E and F, EMSA assays using probes derived from the PBF1 target gene promoters containing P-box-binding sites identified in this study. Unlabeled WT and mutated probes were used as competing DNA fragments. The magenta letters in the labeled probes represent the core sequence of P-box. The magenta letters in mutated probes represent the mutated sequence of P-box.

transcriptional levels of 43 targets are altered by N limitation. Of these, 26 were downregulated and 17 were induced under DN conditions (Figure 7A and Supplemental Data Set S9). For the DN-specific-PBF1-direct-targets, the transcriptional levels of only 23 targets were altered by N deficiency (Figure 7A and Supplemental Data Set S9). We refer to the PBF1 targets regulated by N levels as SN-specific-PBF1-direct-DEGs and DN-specific-PBF1-direct-DEGs.

To understand the functions of the N-dependent PBF1-regulated gene network, we performed GO enrichment analysis on the specific-direct-target-DEGs using the databases agriGO (Tian et al., 2017) and g:Profile (Uku et al., 2019; Figure 7B and Supplemental Data Set S10). For the SN-specific-PBF1-direct-DEGs, 10 PBF1-activated zein genes were associated with the most enriched molecular function GO term "nutrient reservoir activity." Of these, nine were downregulated under DN conditions (Supplemental Data Set S9). Five PBF1 direct target DEGs were enriched in the "cellular amino acid metabolic process"; their expression was altered by N limitation. In addition, we observed that N deficiency significantly affected cellular carbohydrate metabolism, as evidenced by the enrichment of categories such as

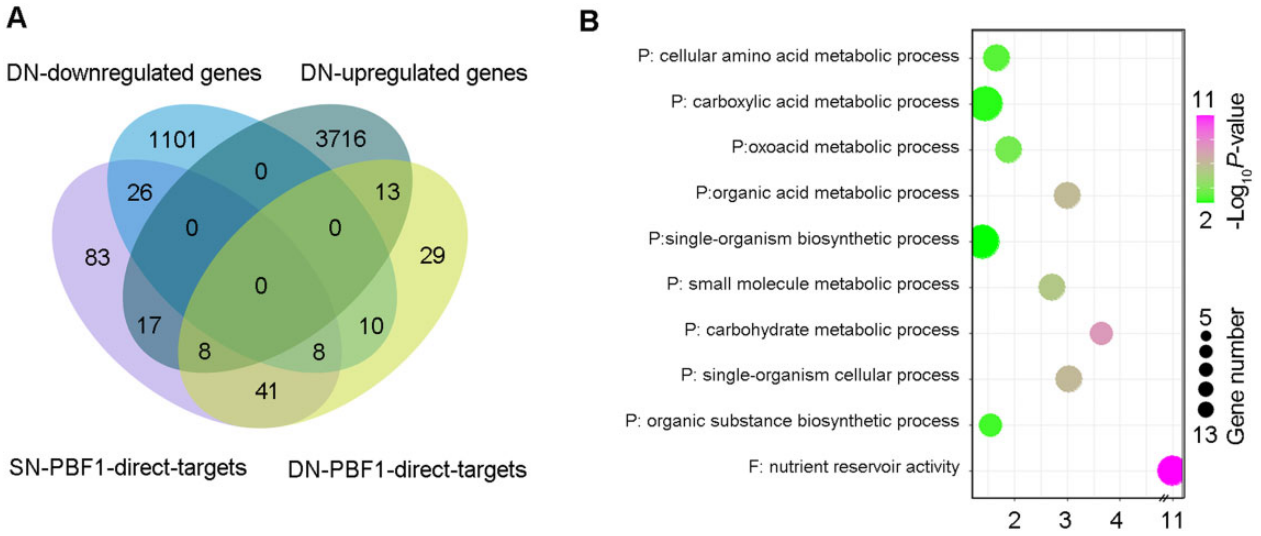

Figure 7 The biological functions of SN-specific-PBF1-direct-DEGs based on GO term enrichment analysis. A, Venn diagram showing the overlap of DEGs regulated either by PBF1 or by N limitation (identified by RNA-seq) and PBF1 target genes (identified by ChIP-seq). B, GO term classification of SN-specific-PBF1-direct-targets. The size of circles is scaled to the number of SN-specific-PBF1-direct-target enriched in the GO terms. F, molecular function; P; biological process.

"oxoacid metabolic process," "starch catabolic process," "carboxylic acid metabolic process," "carbohydrate catabolic process," and "cellular glucan metabolic process" (Figure 7B). Ten SN-direct-target-DEGs were enriched in these GO terms (Supplemental Data Set S10). Among these genes, eight PBF1-repressed targets were significantly upregulated genes in DN endosperm, including *Su1*, *Sbe1* (encoding the critical starch biosynthesis enzymes), and *Pyk2* (encoding pyruvate kinase). Consistent with this observation, the expression levels of *Su1* and *sbe1* were significantly upregulated by 94.9% and 113.6%, respectively, in the *pbf1RNAi* plants (Zhang et al., 2016). In addition to *Su1* and *sbe1*, the five remaining genes enriched in the above GO terms were also upregulated by 62.1%–175.0% in the *pbf1RNAi* plants (Zhang et al., 2016). These results suggested that PBF1 has a positive effective on the biosynthesis of N compounds (zein proteins), but a negative effective on C metabolism under SN conditions. In addition, two SN-direct-target-DEGs involved in organ development, *Zar5* (*Z. mays ARGOS1*, encoding an auxin-regulated gene involved in organ size) and Zm00001d025872 (senescence regulator) were also downregulated by N deficiency. This result indicated that organ development regulated by PBF1 may depend on N availability. Due to the small number of DN-specific-PBF1-direct-DEGs (26 genes), we identified no significant enrichment GO terms.

Among the 57 common-PBF1-direct-targets, 41 genes not only were bound by PBF1 under both SN and DN conditions but also showed stable expression under both conditions (Figure 7A, Supplemental Figure S15, and Supplemental Data Set S9). Although no GO terms were enriched in biological processes categories, several important genes were identified in the dataset, including *PPDK1*, *27-kD γ-zein*, *Bt1*, and *ZmWCR1* (Supplemental Data Set S9). The expression of *27-kD γ-zein* was also not significantly altered between SN and DN conditions ($\log_2$ fold change [DN/SN] = 0.47; false discovery rate [FDR] = 0.44; Supplemental Table S2, Supplemental Figure S16). *Bt1* is associated with ADP-glucose transport into endosperm plastids and plays an important role in starch biosynthesis (Kirchberger et al., 2007). The transcript level of *Bt1* was not significantly different between SN and DN conditions ($\log_2$ fold change [DN/SN] = 0.57; FDR = 0.54). *ZmWCR1* is the maize homolog of *OsWCR1* in rice (*Oryza sativa*). Os*WCR1*, F-box genes, is regulated by OsDOF17 to negatively regulate grain chalkiness and improve grain quality (Wu et al., 2022). We determined that the *ZmWCR1* gene was bound and modulated by PBF1 under both SN and DN conditions, and its transcriptional level was not significantly altered by N deficiency ($\log_2$ fold change [DN/SN] = −0.58; FDR = 0.93). As a result, most of the common-PBF1-direct-targets are less influenced by N supply. That is, the differential expression of PBF1 target genes under different N levels is mainly achieved through presence or absence of binding by PBF1 between SN and DN conditions.

In maize, PPDK2 accounts for the large majority of endosperm PPDK activity, whereas PPDK1 is specified for abundant mesophyll form (Méchin et al., 2007; Lappe et al., 2017). This is consistent with our observation that the TPM value of PPDK2 is ∼4- to 6-fold that of PPDK1 under SN conditions (Supplemental Figure S16). At 15 DAP, transcripts of *PPDK2*, whose promoter was bound by PBF1 only under SN conditions, were slightly less abundant in B73 endosperm under DN conditions (TPM = 2521.6) compared to SN conditions (TPM = 2896.7), yet it was not a significant DEG ($\log_2$ fold change [DN/SN] = −0.20; FDR < 0.05). The same result held true for the expression of *PPDK2* at 24 DAP, albeit with a much lower expression level than that at 15 DAP. In contrast to *PPDK2*, the expression level of *PPDK1*

was higher in B73 endosperm under DN conditions at 15 DAP (Supplemental Figure S16). Again, it is uncertain whether the difference was significant due to the high FDR value (SN-TPM = 472.2, and DN-TPM = 930.2; FDR = 0.12). Moreover, the elevation (if any) in expression level of *PPDK1* would be accompanied by a reduction of that of *PPDK2* (Supplemental Figure S16), so the overall expression level of *PPDKs* may remain comparable the endosperms grown under between DN conditions and SN conditions.

Relationship between PBF1 binding and expression of *zein* genes under different N conditions

Products from three zein subfamilies (27-kD γ-zein, 22-kD α-zein, and 19-kD α-zein) account for more than 70% of the total amount of zein in the kernels (Wu and Messing, 2014). We examined the PBF1-binding pattern to these *zein* genes under SN and DN conditions (Figure 8A). We observed that PBF1 binds to the promoters of six *22-kD α-zein* genes (induced target genes) and seven *19-kD α-zein* genes (three induced genes, one repressed gene, and three bound genes with stable expression) in the SN endosperm. Among the SN-PBF1-direct-targets, one *22-kD α-zein* gene was upregulated, and the other α-zein genes (5 *22-kD α-zein* and 7 *19-kD α-zein*) were downregulated under N deficiency. It is worth noting again that the *27-kD γ-zein* was bound by PBF1 under both SN and DN conditions (Supplemental Table S6). Based on our RNA-seq and RT-qPCR data, the expression levels of *27-kD γ-zein* did not change significantly in response to N deficiency (Supplemental Figure S7 and Supplemental Figure S16), suggesting distinct responses of different *zein* genes to N limitation.

To confirm whether the binding sites in the *zein* promoter regions were bound by PBF1, we selected seven sites for ChIP-qPCR analysis (Figure 8B, Supplemental Table S5, and Supplemental Figure S17). Except for the site for *Z1D-4* (encoding one of 19-kD zein), all sites were enriched under SN conditions. Among them, the site in *18-kD δ-zein* promoter was the most enriched in the ChIP SN-WT DNA, followed by *Z1C-10*, which was enriched by nearly 5-fold enrichment under SN conditions. *Z1B-5* was the least enriched site (by 2.3-fold) under SN conditions. However, only the sites of in the *27-kD γ*-zein and *50-kD γ-zein* promoters were enriched under DN conditions (Figure 8B and Supplemental Figure S17). The ChIP-qPCR data confirmed the specific association of PBF1 with the identified genomic regions under SN conditions, suggesting that the lack of PBF1 binding correlates with the lower expression of some *zein* genes under DN conditions. Furthermore, the SDS-PAGE analysis of zein accumulation at 15 DAP was consistent with this result. We observed a pronounced decrease in abundance of 22-kD and 19-kD α-zein under DN conditions compared with that under SN conditions, whereas 27-kD γ-zein abundance remained relatively constant in DN and SN endosperm (Figure 8, C and D). Thus, to a certain degree, the binding of PBF1 to a promoter sequence around TSSs might influence the expression of downstream *zein* genes and alter the abundance of some zein proteins under different N conditions.

Transcriptional activation and repression of genes related to N and C metabolism by PBF1

According to previous studies, Dof family numbers can be activators and/or repressors of their targets (Gupta et al., 2015). To test whether PBF1 functions as a transcriptional activator or a repressor of its target genes, a transient transcription dual-luciferase assay was performed in *Nicotiana benthamiana* leaves, using *Pbf1* driven by the cauliflower mosaic virus (CaMV) 35S promoter as an effector and LUC (the coding region of firefly luciferase) driven by the different gene promoters as reporters (Figure 9A). Consistent with previous studies showing that PBF1 regulates *27-kD γ-zein* (Zhang et al., 2016), coexpression of the reporter (*27-kD γ-zein*) with the effector (35S:*Pbf1*) resulted in a 7-fold increase in LUC activity compared with the control (empty vector, NC). In addition to the promoter of the *zein* gene, we also performed the same assay with the promoter sequence of Zm00001d027536 (encoding serine acetyltransferase4), which was downregulated in *pbf1*-endosperm (Supplemental Data Set S8). Significant expression of LUC, but not as dramatic as that for *27-kD γ-zein*, was detected for the promoter of Zm00001d027536 and PBF1 (Supplemental Figure S18). This suggested that PBF1 binds and activates genes encoding storage proteins and enzymes involved in amino acid biosynthesis or metabolism in maize endosperm in an N-dependent manner.

Nearly two-thirds of the SN-specific-PBF1-direct-targets (79/126) were upregulated in the *pbf1* endosperm, for which there was no PBF1 binding due to the absence of PBF1 (Supplemental Data Set S5). Accordingly, we speculated that PBF1 represses the expression of genes in the SN endosperm, many of which are involved in starch synthesis. We also performed the same assay with the promoter sequences of several starch synthesis genes, including *Su1, Sbe2b, Bt1, and Pho1*. Consistent with this notion, the transient assay in *N. benthamiana* leaves showed that 35S-PBF1 reduced the LUC activity driven by those promoters more than that with the same reporter and the empty vector (Figure 9).

A previous study observed that ZmbZIP22 positively regulates the expression of starch synthesis genes in endosperm (Chen et al., 2015). In addition, ZmbZIP22 can interact with PBF1 (Li et al., 2018). Therefore, when we coexpressed the two TF genes in a transactivation assay (Figure 9), ZmbZIP22 alone transactivated the promoters of *Su1, Sbe2b, Bt1, and Pho1* but coexpression of PBF1 and ZmbZIP22 repressed the promoters of *Su1, Sbe2b*, and *Pho1* (Figure 9). ZmbZIP46, which has strong sequence similarity to ZmbZIP22, transactivated the promoters of *Su1* and *Sbe2b* (Supplemental Figure S19). Similarly, when ZmbZIP46 was coexpressed with PBF1, the transactivation activity of ZmbZIP46 toward the *Su1* and *Sbe2b* promoters was significantly repressed by PBF1(Supplemental Figure S19). Taken together, these results suggest that PBF1 can behave not

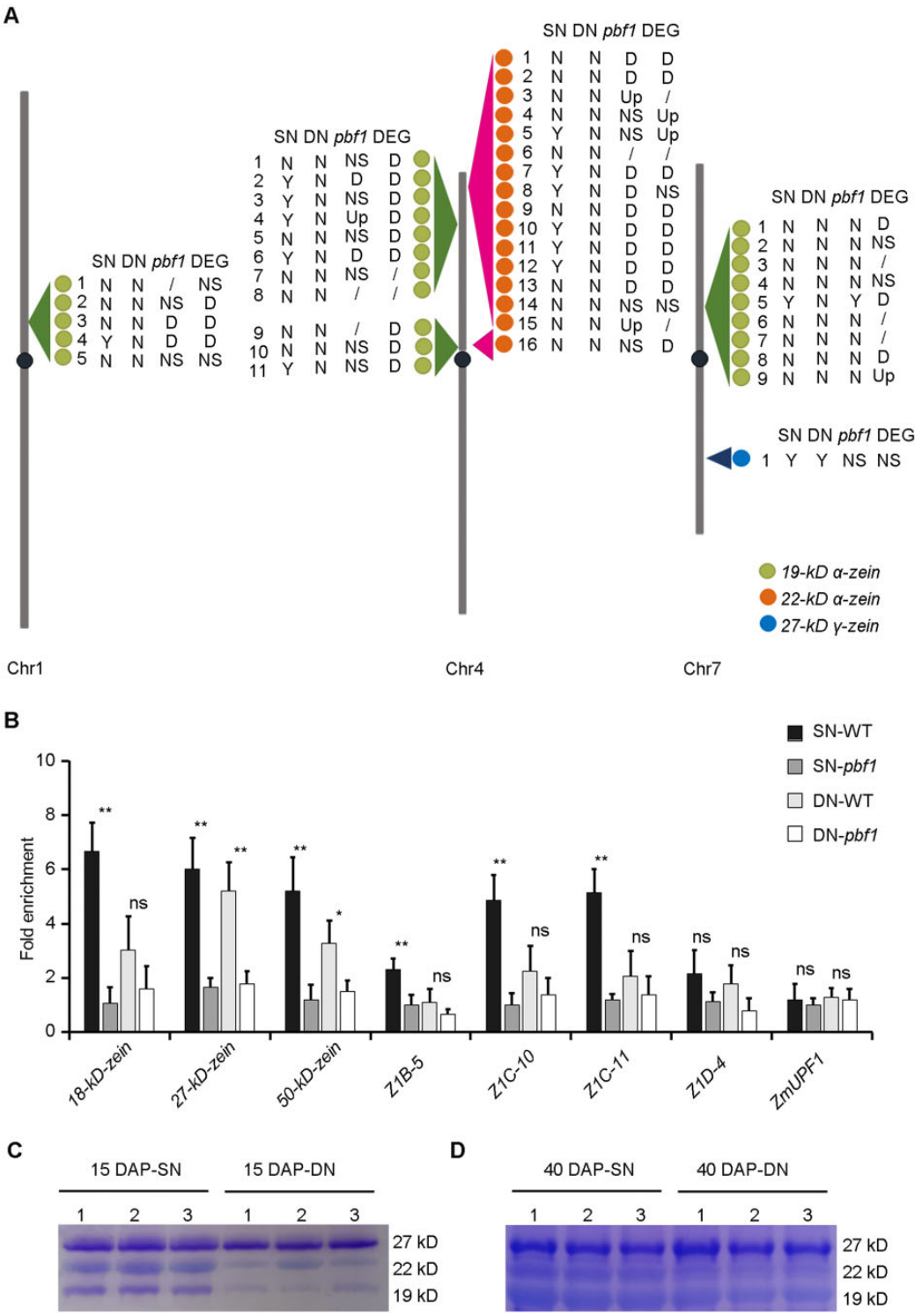

Figure 8 Differential binding of PBF1 to zein genes under SN and DN conditions. A, The binding patterns of 19-kD α-, 22-kD α- and 27-kD γ-zein genes under different N conditions. SN, ChIP-seq analysis under SN conditions; DN, ChIP-seq analysis under DN conditions, *pbf1*, PBF1-regulated DEGs, DEGs N-regulated DEGs. Y, PBF1-bound target. N, a non-PBF1-bound target. D, the expression of this gene was down regulated under DN conditions compared with SN conditions; Up, the expression of this gene was up regulated under DN conditions compared with SN conditions; NS, non-DEGs. Vertical bars represent the maize chromosomes. Chromosomes 1, 4, and 7 are indicated from left to right. B, ChIP-qPCR assays confirming the in vivo binding activity of PBF1 to the promoter region of zein genes under SN and DN conditions. Data are shown as mean ± SD of three biological replicates from three different ears. Significant differences were determined using Student's *t* test. $^{*}P < 0.05$,$^{**}P < 0.01$. ns, not significant (Supplemental Data Set S13). C and D, Coomassie Brilliant Blue staining of SDS-PAGE gels from 15 DAP (C) and 40 DAP (D) endosperm collected from KN5585 plants grown under SN or DN conditions.

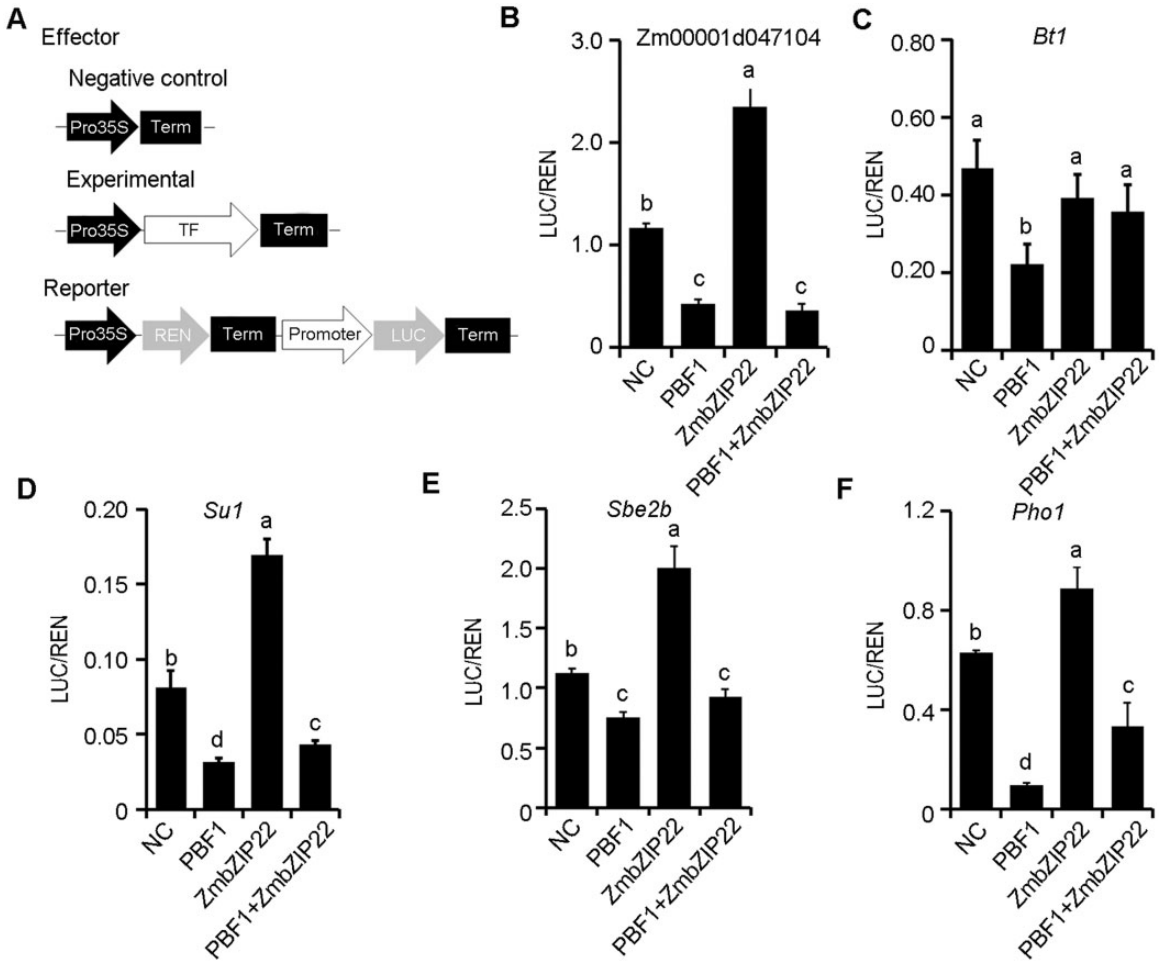

Figure 9 PBF1 as a transcriptional repressor. A, Schematic diagrams of the effector and reporter constructs. "REN" represents Renilla luciferase; "LUC", firefly luciferase; "Term", terminator. "Pro35S", the promoter of CaMV 35S; "TF", the cDNA of TF, "Promoter", the promoter of target gene. B–F, Transient activation of the Zm00001d047104, *Bt1*, *Su1*, *Sbe2b*, and *Pho1* promoters driving LUC reporter gene, respectively. PBF1, overexpressed PBF1, ZmbZIP22, overexpressed ZmbZIP22, PBF1 + ZmbZIP22, coexpressed PBF1 and ZmbZIP22. *Nicotiana benthamiana* leaves were infiltrated with the LUC reporter and the indicated effectors. Renilla (REN) activity was used as an internal control. NC, empty vector. The LUC/REN ratio represents the relative activity of target promoters. Three independent experiments were performed from different plants. Data are average values ± SD of three independent experiments. Different lowercase letters mean significant difference between treatments, as determined by Duncan's multiple-comparison tests ($P < 0.05$; Supplemental Data Set S13).

only as a transcriptional activator but also as a repressor for its target genes.

PBF1 and O2 cooperate to regulate target genes

O2 and PBF1 cooperatively promote the activation of most O2 targets, such as a number of zein genes, *PPDK1/2* and *SSIII* (Vicente-Carbajosa et al., 1997; Wu and Messing, 2012; Zhang et al., 2016). To investigate the gene regulatory network co-modulated by PBF1 and O2 in developing maize endosperm, we compared the peaks derived from two independent O2 ChIP-seq datasets (Li et al., 2015; Zhan et al., 2018) with the peaks identified in the PBF1 ChIP-seq assay from this study. We observed 215 common genes (associated with 305 peaks) bound by both PBF1 and O2 (Figure 10, A and B), and 112 of them contained the O2 box in their promoter regions (Supplemental Data Set S11). Therefore, the common binding targets only account for a small portion of the genes bound by either O2 or PBF1.

Among the targets, 42 genes were directly regulated by O2, whereas only 8 genes were directly modulated by PBF1, such as some zein genes, *PPDK1/2*, and genes related to responses to stress (such as Zm00001d035558). The remainder of the O2 direct target genes were bound by PBF1, but the expression of those genes was not significantly altered in *pbf1* mutants. Some of those genes are involved in carbohydrate metabolic processes (such as *Sh1* and two genes encoding xyloglucan endotransglucosylase/hydrolase), seed development (*ZmPPR* and *ZmNKD2*), and genes related to stress responses, such as *Adh1* (Figure 10C). In addition, the set of PBF1-O2-bound genes included several genes encoding important TFs, such as *ZmNAC130*, *ZmNAC87*, *ZmbZIP34* and *ZmNKD2*. *Zm*NKD2 is involved in regulating

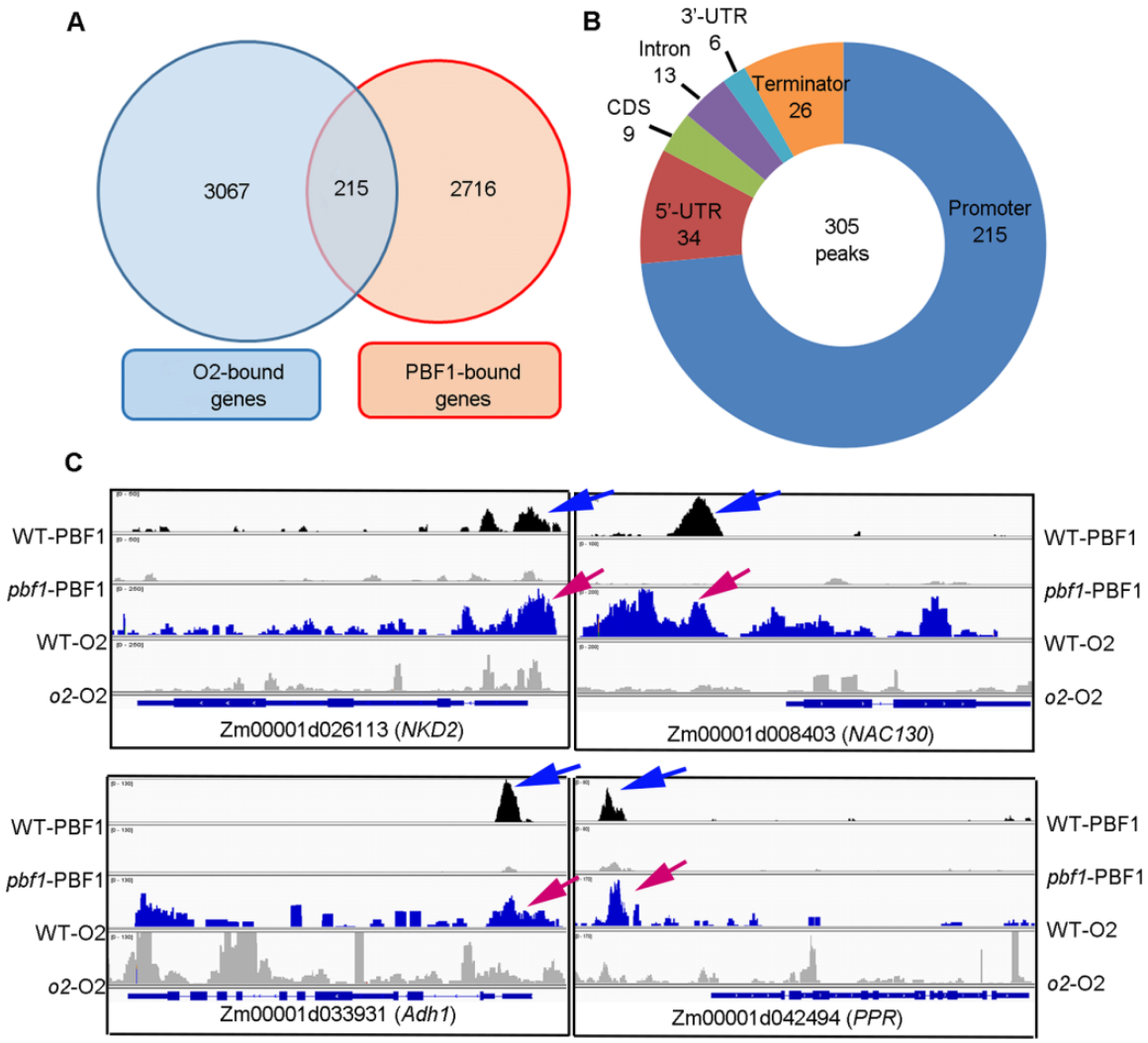

Figure 10 The regulatory network of PBF1 and O2 in the maize endosperm. A, Venn diagram showing the overlap between the genes whose promoters are bound by O2 (Li et al., 2015; Zhan et al., 2018) and those whose promoters are bound by PBF1 in SN endosperm. B, Distribution of peaks mapping to the overlapping genes bound by both O2 and PBF1 under SN conditions in the maize genome. C, Visualization of ChIP-seq reads and peaks of SN PBF1 and O2-binding sites for four gene loci using the Integrated Genome Viewer. Blue arrows indicate overlapping peaks of PBF1. Magenta arrows indicate overlapping peaks of O2 (Li et al., 2015; Zhan et al., 2018).

many endosperm developmental processes (Gontarek et al., 2016). These results suggest that PBF1 indeed jointly regulates a few genes with O2 but the main regulatory spectrum for the two genes is largely independent.

Discussion

Variation in N availability in the environment triggers complex effects on proteins and starch deposition in maize seeds. Previous studies showed that N limitation substantially affects the C and N contents in kernels (Singletary and Below, 1989; Singletary et al., 1990). In this study, we demonstrated that N deficiency led to increased starch contents with reduced protein contents in both the developing and mature endosperms (Figure 1). RNA-seq analysis showed that the expression of many N and C metabolism-related genes was altered by N deficiency. Loss of PBF1 function affected the transcript level of numerous genes involved in C and N metabolism (Figure 3B), and the expression levels of most of these genes were altered by changes in the N level as well (Figure 3C). The combination of RNA-seq and ChIP-seq analyses showed that the spectrum of PBF1 target genes changed in the developing endosperm depending on N conditions (Figure 5). PBF1 interacted with the promoters of a subset of these genes, resulting in transcriptional activation or suppression, results consistent with those from a previous study (Zhang et al., 2016). Thus, the presence/absence of PBF1 at upstream of its target genes is a major factor responsible for altered expression of genes involved in accumulation of storage proteins and carbohydrates under different N conditions.

PBF1 regulates the deposition of storage compounds in endosperm depending on N levels

Using ChIP-seq and RNA-seq analysis, we observed that several starch synthesis-related genes were directly bound and

regulated by PBF1, including *Su1*, *Pho1*, *Sbe2a*, and *Sbe2b* (Supplemental Data Set S9). Moreover, the expression of those genes was altered by changing the N levels. Isoamylase 1 (ISA1), encoded by *Su1*, is vital for ensuring the correct formation of starch granules because it trims nascent amylopectin to generate malto-oligosaccharides (MOSs), and MOSs are required as primers for starch synthesis (Kubo et al., 2010; Seung and Smith, 2018). Loss of function of ISA results in reduced starch content, abnormal amylopectin structure, and altered starch granule morphology (Du et al., 2018). SBE2b and SBE2a play a major role during amylopectin biosynthesis in cereal endosperm (Liu et al., 2009; He et al., 2020). PHO1 has been reported to combine with SBEs to promote the extension of MOSs and the synthesis of branched glucans in maize (Subasinghe et al., 2014).

As detailed in results, the starch content in *pbf1* endosperm was higher compared with that in WT endosperm (Supplemental Figure S5B) under SN conditions, and the lack of statistical significance was likely an artifact of the overall high starch content in maize kernels. This is consistent with the notion that PBF1 binds to specific starch synthesis genes and suppresses their expression, thus limiting starch synthesis upon sufficient N supply. In contrast to the starch content, the protein content of the *pbf1* mutants was significantly lower than that in WT plants grown under both DN and SN conditions (Supplemental Figure S5D), indicating that PBF1 has a positive effect on protein synthesis. This was consistent with previous studies showing that PBF1 activates the transcription of *27-kD γ-zein* and *22-kD* α-zein (Wu and Messing, 2012; Zhang et al., 2016). The amplitude of variation in C and N deposition compounds between SN-WT and DN-WT endosperm was greater than that between SN-*pbf1* and DN-*pbf1* endosperm (Figure 2). Therefore, PBF1 may regulate the accumulation of storage compounds in endosperm in response to N levels.

Interaction between PBF1 and target genes modulates by N supply in the developing endosperm

Based on our ChIP-seq analysis, the enrichment of PBF1-binding sites under SN conditions was skewed towards regions adjacent to the TSSs, but enrichment under DN conditions was distributed relatively evenly among different genomic regions (Figure 5A and Supplemental Figure S4), suggesting that PBF1 is more likely to bind to intergenic regions under DN conditions. In Arabidopsis, it was observed that phytochrome B (phyB) is directly associated with the promoters of key target genes in a temperature-dependent manner. Chromatin immunoprecipitation of phyB coupled with sequencing revealed that phyB bound 133 sites at 17°C and 67 sites at 27°C, with 33 shared between 17°C and 27°C (Jung et al., 2016). Thus, PBF1 is not the only TF with a variable spectrum of target genes under different conditions. Compared to the response of phyB to temperature, the response of PBF1 to N supply appears to be more dramatic, with most PBF1 target genes vanishing upon N starvation (Figure 5).

At present, it is unclear how PBF1 switches its binding pattern under different N conditions. Post-translational modifications such as phosphorylation contribute to the capacity of TFs to transactivate downstream target genes. In maize, PBF1 is phosphorylated in the immature endosperm, and dephosphosphorylation using calf intestine phosphatase abolishes its ability of binding to the P-box harbored within the 27-kD γ-zein gene′s promoter (Wang et al., 1998). In this study, we observed that PBF1 was less enriched in the promoter region of the *27-kD γ-zein* gene under DN conditions (Figure 8B), so it is not impossible for a portion of PBF1 to be dephosphorylated upon N deficiency.

On the other hand, studies showed that, under stressed conditions, plant genomes undergo dramatic changes such as methylation/demethylation of genes (Lu et al., 2007; Peng and Zhang, 2009; Li et al., 2014). Some changes tend to make the otherwise condensed chromatin (mostly intergenic regions) accessible, therefore becoming potential-binding sites for PBF1. As a result, more intergenic-binding sites were detected, and the binding sites were distributed more evenly along genomic regions under DN conditions (Figure 5). In addition, more PBF1 recruited to intergenic regions might constitute a mechanism for maize to cope with the N-limitation stress. Because N deficiency had little effect on the expression of *Pbf1*, PBF1 might temporarily bind to the intergenic region under DN conditions in order to slide along the genomic DNA and activate the downstream target genes rapidly once N is available without requiring de novo synthesis of PBF1. In this case, PBF1 may serve as a sentinel protein for N assimilation.

A dual role of PBF1 in regulation of its target genes

Dof TF family members can function as transcriptional activators and/or repressors (Gupta et al., 2015). PBF1 has been identified as a transcriptional activator in previous studies (Wu and Messing, 2012; Zhang et al., 2015; Zhang et al., 2016), yet less is known about its role as a transcriptional repressor. Our analysis indicated that PBF1 functioned as a transcription repressor of several genes involved in starch synthesis in *N. benthamiana* leaves (Figure 9), consistent with a similar assay conducted in Arabidopsis mesophyll protoplasts (Zhang et al., 2016). This corroborates our observation that, under N deficiency, PBF1 was absent from the promoter regions of *Su1* and *Sbe2b*, which were also found to be upregulated by N limitation. The repressive role of PBF1 is in accordance with the elevated expression level of *Su1* in the *pbf1* mutants in our study and the *pbf1RNAi* kernel compared with the WT in the Zhang et al. (2016) study.

It is known that a single TF may differentially regulate its target in plants. In maritime pine (*Pinus pinaster*), PpDof5 activates the transcription of *GS1b* and contributes to the repression of *GS1a* in GUS reporter gene assays, and is proposed to function in nitrogen reassimilation during lignification (Rueda-Lopez et al., 2008). Viviparous 1 (VP1) suppresses the expression of the germination-specific α-

amylase genes in aleurone cells but activates many genes in embryos of developing maize seeds (Zheng et al., 2019). As a result, VP1 plays different tissue-specific roles. In contrast, *Pbf1* mRNA is similar in different portions of the endosperm (Figure 4C), so its variable function on different target genes is unlikely to be attributed to tissue specificity. One possibility is that the distinct promoter sequences for different target genes may create variable conformations of the DNA-protein complex, leading either to promotion or to blockage of transcription of downstream genes. Alternatively, PBF1 interacts with other proteins associated with the target genes, resulting in diverse outcomes on target gene expression.

In maize, ZmDof1 functions as an activator of *C4 phosphoenolpyruvate carboxylase*, but ZmDof2 can inhibit ZmDof1 activity through competing with and interacting with ZmDof1 (Yanagisawa and Sheen, 1998; Yanagisawa, 2000). PBF1 might function as a suppressor of other TFs, such as ZmbZIP91 that positively regulate the expression of *Su1* (Chen et al., 2015). When ZmbZIP22 or ZmbZIP46 was tested alone with the *Su1* and *Sbe2b* promoter, it showed detectable activation activity. Coexpression of PBF1 with ZmbZIP22 or ZmbZIP46 resulted in much less activation activity than ZmbZIP22/ZmbZIP46 alone (Figure 9 and Supplemental Figure S19). These findings suggest that PBF1 acts as a suppressor of ZmbZIP22/ZmbZIP46. Perhaps PBF1 can block the activation activity of ZmbZIP22/ZmbZIP46 through their interaction. We only observed those results with a dual-luciferase activation assay in the *N. benthamiana* leaves (Figure 9 and Supplemental Figure S19). Further biochemical assays and comparative studies are required to reveal the molecular mechanisms underlying the activating and repressing roles of PBF1 as a TF.

PBF1 is a key protein in the starch/protein balance in response to N availability

Because endosperm serves as the energy and nutrition source for the embryo, a rapid response to N supply in synthesis of starch and storage proteins is critical for reproductive success and yield of grain crops. Early studies led to the hypothesis that PPDKs served as the switch for the flux of starch and proteins (Méchin et al., 2007). PPDKs catalyze the reversible conversion of pyruvate, inorganic phosphate (Pi), and ATP into phosphoenolpyruvate (PEP), AMP, and pyrophosphate (PPi). This process provides an important carbon skeleton (PEP) for amino acid synthesis (Chastain et al., 2006). In addition, the PPi generated by the catalytic reaction favor the degradation of ADP-glucose, which is a substrate for starch synthesis (Méchin et al., 2007). Thus, it was proposed that PPDK activity would reduce starch accumulation in favor of amino acid synthesis, and that PPDKs play a central role in the starch-proteins balance (Méchin et al., 2007; Hennen-Bierwagen et al., 2008). This hypothesis is in accordance with the overall reduction of zein content in endosperm of *o2* mutants, since PPDKs seem to be activated by O2 (Prioul et al., 2008). A recent study finds that *PPDK* transcript abundance modulates metabolism through reversible adjustment to energy charge in endosperm. However, PPDK does not seem to control the net division between starch and storage proteins biosynthesis, in that no significant differences in the endosperm starch and total N contents were detected between PPDK-deficient endosperm and normal endosperm (Lappe et al., 2017).

Our comparative analysis using maize plants grown under different N conditions provides a unique opportunity to further examine the role of PPDKs in the production of starch and proteins. In maize, PPDK2 accounts for the majority of endosperm PPDK, whereas PPDK1 specifies the abundant mesophyll form (Méchin et al., 2007; Lappe et al., 2017). According to our RNA-seq and ChIP-seq data, the promoter of *PPDK2* was bound by PBF1 only under SN conditions, and its expression levels remained largely stable or slightly reduced upon N starvation. On the other hand, although *PPDK1* was bound by PBF1 under both SN and DN conditions, its expression levels increased upon N starvation (Supplemental Figure S16). Although the expression level of *PPDK1* in endosperm was only a fraction of that of *PPDK2*, it is questionable whether the variation in *PPDK2* expression would influence the overall PPDK activity in endosperm. Taken together, the lack of dramatic variation in expression levels of *PPDKs* in response to N supply is consistent with the recent view that PPDK is involved in C and N metabolism but is not the master switch between starch and storage proteins biosynthesis in endosperm (Lappe et al., 2017).

Our analyses indicated that PBF1 is likely to play an important role in regulating the starch/protein balance under both SN and DN conditions. This is achieved by differential binding in response to the N supply as well as the regulatory roles of PBF1 (Figure 11). Briefly, under normal N conditions, the binding of PBF1 activates the expression of genes involved in N metabolism and suppresses expression of genes involved in starch synthesis, promoting accumulation of storage proteins. This is consistent with the observation that reduction of zein proteins in *pbf1* mutants is more pronounced under SN conditions than under DN conditions (Supplemental Figure S5D). This also explains the elevated level of starch in *pbf1* mutants. Upon N starvation, PBF1 is released from the majority of its target genes, leading to reduced activity of genes involved in N metabolism and release of suppression of genes related to carbohydrate metabolism, thus enhancing accumulation of starch in endosperm. Meanwhile, PBF1 remains bound to some zein genes, and ensures the synthesis of these proteins to meet the essential nutritional requirements of the seed. In this way, PBF1 allows rapid acclimation to environmental N levels and maximizes the fitness potential of the next generation of maize plants. It is worth mentioning that *pbf1* mutants still respond to N availability, yet to a lesser degree (Figure 2), suggesting the likelihood that other TFs and genes are involved in this process.

Potential application of PBF1 and nitrogen supply in improving maize grain quality

The early filling stage is critical for high grain yield at later stages (Borrás et al., 2009). In this study, we observed that N

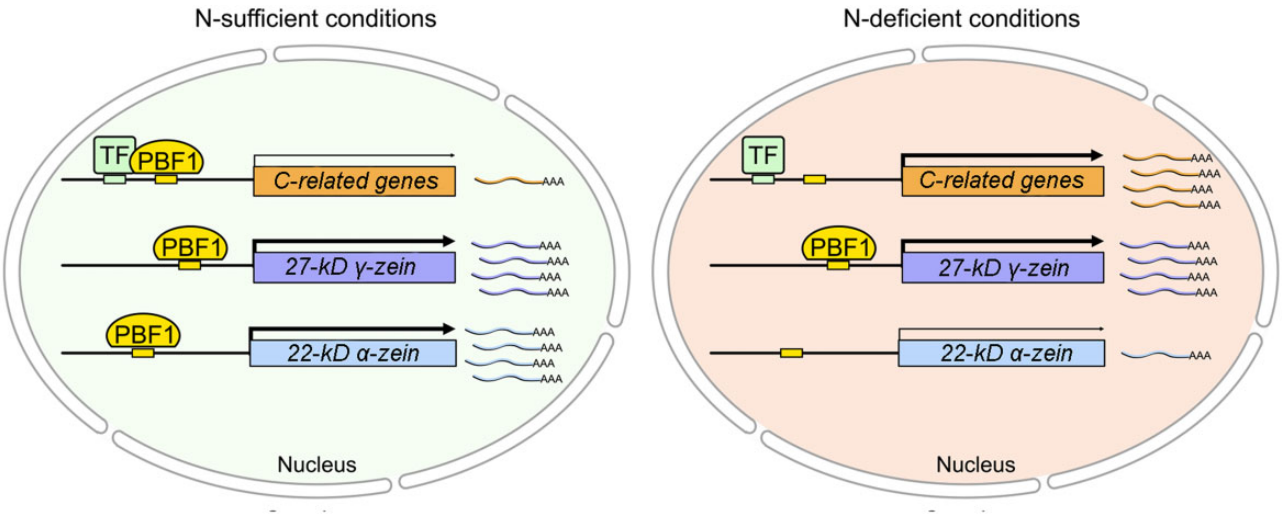

Figure 11 A proposed model for the regulatory network of PBF1 contributing to the balance of protein and carbohydrate storage in maize endosperm cells. Under N-sufficient conditions (left), the binding of PBF1 activates the expression of genes involved in N metabolism and suppresses the expression of some genes (such as *Su1* and *Sbe2b*) involved in starch biosynthesis, thereby promoting the accumulation of storage proteins. Upon N-deficient conditions (right), PBF1 is released from the majority of its target genes, leading to reduced activity of genes in N metabolism and alleviating transcriptional suppression for genes related to carbohydrate metabolism, thus enhancing the accumulation of starch in endosperm. Meanwhile, PBF1 remains bound to some *zein* genes, and ensuring the biosynthesis of these proteins to meet the essential nutrition requirements of the seeds. TSS, Transcription start site.

deficiency led to elevated starch contents and reduced the protein contents from 15 to 40 DAP (Figure 1), suggesting that the synthesis of storage products in early phases may affect the quality and yield of maize kernels. During the process of endosperm development, cell differentiation and mitotic proliferation of the maize endosperm continue to ~16 DAP, a time when endosperm structure is nearly finalized, that is, maize has completed establishment of the reproductive sink at this stage (Becraft and Gutierrez-Marcos, 2012; Leroux et al., 2014; Zhan et al., 2017). At this time, genes related to C and N metabolism begin to be expressed in large quantities. In particular, most zein genes reach their maximum expression levels at this point, directly contributing to the deposition of C and N at the early filling stage (Chen et al., 2014). Thus, proteins and starch begin to be stored in the endosperm in the early filling stage.

In maize endosperm, zein proteins account for over 70% of the total proteins (Wu and Messing, 2014). Cysteine is abundant in 27-kD γ-zein, and can be used to form methionine (Wu and Messing, 2014). Cysteine and methionine are essential amino acids for human nutrition. In contrast, 19-kD and 22-kD α-zein proteins are largely devoid of the essential amino acid residues lysine and tryptophan. In addition, 27-kD γ-zein is crucial for zein protein body (PB) formation because it controls PB initiation, whereas α-zein is only involved in PB filling (Guo et al., 2013). 27-kD γ-zein ensures the successful formation of PB and the efficient accumulation of other zein storage proteins (Guo et al., 2013). Furthermore, 27-kD γ-zein is necessary for forming a hard and vitreous endosperm to avoid pest and disease attacks (Liu et al., 2016), especially for kernels grown under DN conditions. Thus, a stable level of 27-kD γ-zein protein is important for both kernel nutritional quality and endosperm development. The *o2* mutant has been used to improve kernel nutritional quality, as it reduces the level of zein proteins. When the synthesis of α-zein proteins is reduced, the levels of other seed proteins are increased as a mechanism of compensation, increasing the nutritional value of the seeds (Wu and Messing, 2014).

However, the absence or reduction of zein regulators (O2 and PBF1) significantly reduce the kernel yield. This greatly limits the application of these mutants in breeding. The growth of maize kernels depends on the availability of C and N assimilates supplied by the maternal plant and the capacity of the kernel to use them. One study revealed that under a moderate level of C (292 mM sucrose), maximum kernel growth was obtained when the N supply was raised from 0 to 10 mM (Cazetta et al., 1999). On the other hand, endosperm growth was unchanged but albumin and globulin contents were decreased by additional N supply. When the N level exceeded approximately 72 mM, it reduced starch accumulation (Singletary and Below, 1989), whereas zein protein accumulation increased with the increase in N supply (Singletary and Below, 1989; Singletary et al., 1990). Thus, if the application of N-containing fertilizer is limited to an appropriate level, it is possible to reduce the content of α-zein (therefore increase the nutritional value of the seeds as albumin/globulin was increased) without a dramatic impact on yield. Also, a reduced use of N-containing fertilizer mitigates the negative influence on the environment.

Whereas 27-kD γ-zein protein remained stable under different N levels, the level of α-zein protein dramatically decreased due to N deficiency (Figure 8). Furthermore, PBF1 constitutively bound the promoter of the *27-kD γ-zein*

under both N conditions, but only bound the promoters of few α-*zein* under DN conditions, suggesting that the absence of PBF1 from promoters of these genes may be responsible, at least partially, for the reduced level of α-*zein* upon N starvation. If we could understand more about the mechanism of disassociation of PBF1 with α-zein genes, it could be possible to control the relevant factors so that PBF1 does not interact with α-zein genes even under normal N conditions. In that case, high nutritional quality could be achieved without sacrificing yields. An alternative approach is to directly engineer the PBF1 protein. The DNA binding domain is located at the N-terminal of PBF1 (Marzábal et al., 2008). It would be intriguing to mutate the DNA binding domain of PBF1 to test whether it is possible to retain its binding activity to *27-kD γ-zein* with a reduced affinity to α-zein genes. Taken together, a greater understanding of the interactions of PBF1 and its target genes may allow the development of maize varieties with high nutritional value and stable yield.

Materials and methods

Plant material and culture

Maize (*Z. mays*) *Pbf1* CRISPR-Cas9 transgenic lines (in the KN5585 background) were generated by WIMI Biotechnology Company. The 20-bp guide RNA target editing sequence was selected in the second exon of PBF1. Eleven CRISPR/Cas9 edited plants were crossed with KN5585 inbred lines to obtain construct-free materials (Supplemental Data Set S12). The mutants (*pbf1-1* and *pbf1-2*) were backcrossed to the KN5585 genetic background for three generations, and then the positive plants were self-pollinated for two generations, yielding the homozygous *pbf1* mutants. The maize inbred KN5585 (WT) was used as negative control.

The field experiment was conducted at the Luhe Experimental Station (32°12′N, 118°37′E), Nanjing, China. The N-deficient soil used possessed only 0.76 g N kg^{-1} of extracted mineral N, together with 26.5 mg kg^{-1} of available phosphorus (P), 72.4 mg kg^{-1} of available potassium (K), and 12.8 g kg^{-1} of organic matter. According to previous studies (Liao et al., 2012; Pan et al., 2015), N treatments were applied over the entire growth period to make available either a minimal (0 kg N/ha supplemental; deficient N, DN) or an optimal N supply (240 kg N/ha; sufficient N, SN) in the form of ammonium sulfate in this study. For the DN treatment, the pre-sowing base fertilizers were 135 kg P_2O_5 ha^{-1} and 80 kg K_2O ha^{-1}. Another 40 kg ha^{-1} of K_2O was applied at the silk stage. For SN treatment, N fertilizer was applied at rates of 70, 100, and 70 kg N ha^{-1} at the pre-sowing, V8, and V12 stages, respectively. P and K fertilizers were applied to the SN treatments at similar dosage that was used in the DN treatment.

A randomized complete block design with three replications for each treatment was used in this study. The maize inbred lines B73, KN5585, and *pbf1* mutants were planted in three rows per plot, and each row was 200-cm long with a row spacing of 50 cm. Kernels from plants grown under SN and DN conditions were collected for subsequent analysis at 15 DAP (developing stage), 18 DAP, and 40 DAP (mature stage), respectively. The immature kernels were immediately frozen in liquid nitrogen and stored at −80°C until being used for RNA and protein extraction. Samples were collected from three individual plants for each stage. WT *N. benthamiana* plants were grown in the greenhouse at 23°C and 70% relative humidity under 16-h light (white fluorescent lamp, 20,000 LUX) and 8-h dark photoperiod.

Genotyping

We extracted genomic DNA using the cetyltrimethylammonium bromide (CTAB) method (Murray and Thompson, 1980). The CRISPR-Cas9 targeted site was amplified from genomic DNA using specific primers (Supplemental Data Set S12), and the PCR products were sequenced by Sanger sequencing for genotyping.

Measurement of proteins, free amino acids, starch, soluble sugars contents

At least 30 B73 kernels at the developing and mature stages and the CRISPR/Cas9 transgenic kernels at the mature stage were harvested from plants grown in SN or DN conditions, respectively. The endosperms were separated from the embryos and pericarps. All endosperm samples were heat treated at 105°C for 30 min, dried at 70°C until reaching a constant weight, and then weighed and ground into powder at room temperature for subsequent analysis.

Preparation of total protein from developing and mature maize seed was previously described by Bernard et al.(1994). Zeins and non-zeins were prepared from maize as previously described by Wallace et al. (1990). Levels of total proteins, zein, and non-zein proteins were measured using a BCA Protein Assay Kit (Beyotime Institute of Biotechnology) following the manufacturer's protocol. SDS-PAGE was performed using 15% (w/v) polyacrylamide gels, and the gels were stained with Coomassie Brilliant Blue R250.

Amino acid concentrations were measured using an automatic amino acid analyzer L-8800 (L -8800, Hitachi Instruments Engineering, Tokyo, Japan) using a previously described protocol (Deng et al., 2017). Starch content was measured with the Total Starch Assay Kit (K-TSTA; Megazyme) according to the manufacturer's protocol and adapted as previously described (Feng et al., 2018). Soluble sugars were extracted with 75% (vol/vol) ethanol and measured by the anthrone method (Wang et al., 2013). Each assay above was independently performed 3 times using the endosperms collected from three different ears of plants grown under SN or DN conditions.

Zein annotation and RNA-seq data analysis

There are 41 α-, 1 β-, 3 γ-, and 2 δ-zein genes in the B73 genome (Xu and Messing, 2008). According to Chen's methods (2014), we first confirmed the gene models by mapping publicly available full-length complementary DNAs of zein subfamily genes to B73 bacterial artificial chromosomes and then mapped these back to the current B73 V4 reference

genome (Jiao et al., 2017). We annotated all the possible zein genes in the V4 reference assembly, and found 47 zein genes (41 α-, 1 β-, 3 γ-, and 2 δ-; Supplemental Table S1).

Total RNA was extracted from B73 and the CRISPR/Cas9 transgenic endosperm at developing stage (15DAP) using the SV Total RNA Isolation System (Promega, Madison, WI, USA) according to the manufacturer's instructions. Three biological replicates from three ears were used. From each sample, 10 μg total RNA was used for library construction according to the manufacturer's instructions (Illumina). Libraries were sequenced using an Illumina HiSeq 2500 platform to generate 150 nucleotide paired-end sequence reads. Read quality was evaluated using FastQC software (De Sena Brandine and Smith, 2019) and reads were trimmed to 100 nucleotides to remove low-quality bases with the fastx_trimmer program within the FASTX toolkit (http://hannonlab.cshl.edu/fastx_toolkit/index.html). Only reads with a read length greater than 50 bp were kept for downstream analysis. The high-quality reads were aligned to the cDNA sequence file (downloaded from www.maizegdb.org) derived from Maize B73 genome annotation (V4) using Salmon software (version: 1.1.0). The software (version: 1.1.0) was also used for mapping reads to the reference cDNA sequences and for calculating the transcripts per million (TPM) mapped reads of each transcript using quasi-mapping method (Schurch et al., 2016). The *P*-value of differential expression of each gene was calculated using the EdgeR package (version: 4.0; Robinson et al., 2010). Genes with TPM >1 were used for differential expression analysis, and the significant DEGs were assessed on two criteria: false discovery rate (FDR; *q*-value after adjusting for false discovery rate) $\leqslant 0.05$ and $|\log_2 \text{fold change}| \geqslant 1$, and significant DEGs of zein and starch synthesis genes were assessed when $P \leqslant 0.05$ (Student's *t* test).

Real-time PCR analysis

Total RNA was extracted from B73 and the CRISPR/Cas9 transgenic endosperm at different stages (15 DAP, 18 DAP, and 24 DAP) under SN and DN conditions. We used 1 μg of total RNA for reverse transcription using the PrimeScript TM RT reagent Kit with gDNA Eraser (Takara (Beijing, China) Co. Ltd.; code No. RR047A). Quantitative RT-PCR (RT-qPCR) was performed on a Roche Light Cycler 2.0 with Light Cycler software (build 4.1.1.21) as described previously (Du et al., 2020). Briefly, 1 μL of cDNA was added to 5 μL of SYBR Premix Ex TaqTM (TaKaRa Bio Inc., Japan), together with 0.8 μL of each gene-specific primer (forward and reverse, at 10 mM), and the final volume was brought to 10 μL with DNase-free water. Specific primers for tested genes are listed in Supplemental Data Set S12. The maize gene *ZmUPF1* (Zm00001d006438) was used as an internal control. The RT-qPCR analysis was repeated in three independent experiments.

Preparation of antibodies and immunoblot analysis

The full-length cDNA of P*bf1* was cloned into the pCold vector (TaKaRa), respectively, and the construct transformed into the *Escherichia coli* BL21 strain (Shanhgai Weidi Biotechnology Co., Ltd). Cells were grown at 16°C and induced by the addition of isopropylthio-β-galactoside (IPTG) to a final concentration of 0.8 mM when the optical density at 600 nm reached 0.6. The 6 × His fusion recombinant protein was purified with His-tag Protein Purification Kit (Beyotime, Shanghai, China). Anti-PBF1 antibodies were produced in rabbits by Abclonal Biotechnology (Wuhan) Co., LTD.

Total proteins were extracted from 15 DAP maize endosperms that were grown under SN or DN conditions, respectively. Immunoblot analysis was performed according to a method described by Yang et al.(2021). Subsequently, the interaction between antibody and all the proteins was visualized on immunoblots using an anti-PBF1 antibody. The anti-PBF1 antibody was used at dilution of 1:1,000. The anti-H3 antibody (Sigma-Aldrich, H0164-200UL) was used at the dilution of 1:3,000. Secondary antibodies were goat anti-rabbit IgG-horseradish peroxidase (HRP; Abclonal, AS014), and were used the dilution of 1:5,000.

RNA in situ hybridization

The specific fragment of *Pbf1* was amplified using cDNA as template, and was inserted into the pGEM-T Easy vector (Promega, Madison, WI) for sequencing. According to the method of Zhang (2015), the sense probe was then generated using primers T7-PBF1-F and PBF1-R, and the antisense probe using primers PBF1-F and T7-PBF1-R Supplemental Data Set S12). Sense and antisense probes were transcribed in vitro from the T7 promoter with T7 RNA polymerases using the digoxigenin RNA-labeling kit (Roche, Basel, Switzerland). Fifteen DAP B73 seeds from plants grown under SN and DN conditions for in situ hybridization were fixed and embedded in Paraplast Plus (Sigma-Aldrich, St. Louis, MO, USA) embedding medium. Nonradioactive RNA in situ hybridization with digoxigenin-labeled sense and antisense probes was performed on 10-μm sections of tissues as described by Coen et al. (1990).

ChIP-seq and ChIP-qPCR

ChIP using a PBF1-specific antibody with pooled SN or DN endosperm was performed as previously described (Saleh et al., 2008; Li et al., 2015; Komar et al., 2016). The 15 DAP endosperms of KN5585 and *pbf1* mutants were harvested at the same time as those used for RNA-seq. Three biological replicates prepared under SN and DN conditions were performed. Briefly, dissected endosperms were immediately cross-linked in PBS buffer containing 1% formaldehyde on ice under vacuum for 15 min, after which the vacuum was released and reapplied for another 10 min. Fixation was stopped by infiltrating 2 M glycine (final concentration = 0.125 M) under vacuum for an additional 10 min. The cross-linked endosperms were washed 3 times with sterile ddH_2O and ground into powder in liquid N_2, followed by isolation of nuclei. Nuclear-enriched extracts were resuspended in nuclei lysis buffer (50 mM HEPES PH 7.5, 150 mM NaCl, 1 mM EDTA, 0.3% SDS, 0.1% sodium deoxycholate and 1% Triton X-100, 2 μg/mL pepstatin A, 2 μg/mL aprotinin, and 1

mM PMSF), followed by sonication 24 cycles (15 ON/45 OFF) with Bioruptor Pico. Dynabeads Protein A/G (Invitrogen) and a PBF1-polyclonal antibody that was produced in rabbits by Abclonal Biotechnology (~10 μg) were used to precipitate the DNA, the *pbf1* mutant DNA was used as a control. The precipitated DNA was digested by RNase A and proteinase K and subsequently extracted with phenol: chloroform: IAA (25:24:1).

For ChIP-seq, ChIP-DNA libraries of two biological replicates were constructed and sequenced by Hanyu Biotechnology (Shanghai) Co., Ltd. Briefly, ChIP-DNA samples were end-repaired, followed by A-base addition and ligation with adapters using TruSeqPECluster Kit (Illumina). After PCR enrichment, the DNA libraries were quantified with Qubit (Thermo Fisher), followed by sequencing with an Illumina HiSeq 2500. ChIP-seq reads from the replicate treatments and the replicate controls were aligned against the B73 reference assembly (V4) using Bowtie2 (Langmead et al., 2009). Mapped reads of the biological replicates from SN and DN conditions were subsequently merged, respectively. MACS 2.0 (Zhang et al., 2008) with the cutoff $P < 0.001$ was used to identify enriched peaks in treatments and controls. The annotated gene models related to those peaks detected at the regions between −2 kb ahead of the transcription start sites (TSSs) and + 100 bp after TSSs were classified as PBF1-bound targets. To search for conserved binding motifs in PBF1 binding regions, the 400-bp sequence surrounding the peak summit of each consistent peak was extracted and examined using the online version of MEME-ChIP (Machanick and Bailey, 2011; Bailey et al., 2015) with default settings. A custom background model derived from JASPAR CORE (2018) plants was provided, and any number of repetitions of a motif was allowed. The GO enrichment analyses were performed using the database g:Profile (http://biit.cs.ut.ee/gprofiler/; Uku et al., 2019) and agriGO (http://bioinfo.cau.edu.cn/agriGO; Tian et al., 2017).

For ChIP-qPCR, IgG (Abclonal, AC005) was used as the control. The level of each gene in three biological replicates from three ears was normalized to that of *ZmUPF1* measured in the sample. RT-PCR was performed using the SYBR Premix Ex Taq II (Takara) on a LightCycler 484 Real-Time PCR System (Roche). ChIP values were normalized to their respective DNA input values. The fold-changes were calculated using the DCt (threshold cycle) method (Komar et al., 2016). Primers used for ChIP-qPCR are listed in Supplemental Data Set S12.

Electrophoretic mobility shift assay (EMSA)

The cDNA fragment encoding the Dof domain of PBF1 was cloned into vector pET-28a (Novagen). The construct was introduced into *E. coli* BL21 strain (Shanhgai Weidi Biotechnology Co., Ltd). Induction was performed by adding IPTG to a final concentration of 0.3 mM and cells were cultured at 16°C for an additional 24 h. Recombinant proteins were purified using the His-tag Protein Purification Kit (Beyotime, Shanghai, China) and were later used for EMSA.

Oligonucleotide probes were synthesized and labeled with biotin at the 5′-end. The double-strand DNA fragments were acquired by annealing equal molar concentrations of both complementary oligos in 5× annealing buffer (Beyotime, Shanghai, China, D0251). Purified proteins (60 ng) were mixed with 2.5 ng of probe at 25°C for 20 min in an EMSA/Gel-Shift Binding Buffer (Beyotime, Shanghai, China). The mixture was separated by 6% native PAGE in 0.5× TBE buffer. The DNA in the gel was then transferred to N+ nylon membranes (0.2 μm, Millipore, UAS). The DNA on the membranes was detected using the Chemiluminescent EMSA Kit (Beyotime, Shanghai, China) on a Tanon 5200 chemiluminescent Imaging System (Tanon Science and Technology). All oligonucleotides and primers are listed in Supplemental Data Set S12.

Transient expression assay in leaves of *N. benthamiana*

To test the function of PBF1, approximately −1,500 bp upstream regions of the start codon of the PBF1-bound targets were cloned into the vector pGreenII0800-LUC to generate a reporter. The full-length cDNAs of *Pbf1*, *ZmbZIP22*, and *ZmbZIP46* were individually inserted into vector pMDC83-2 × 35S to generate the effectors. Vector pMDC83-2 × 35S was used as the negative control effector. The reporter and the effector were transformed into *Agrobacterium* GV3101(pSoup-p19; Shanhgai Weidi Biotechnology Co., Ltd) and then were infiltrated into the leaves of *N. benthamiana* as described previously (Feng et al., 2018). After incubation in the dark for 24 h and then in the light for 24 h, the firefly luciferase (LUC) activity and Renilla luciferase (REN) activity was measured using the Dual-Luciferase Reporter Gene Assay Kit (Beyotime, Shanghai, China). The ratio between LUC and REN activities was measured in three biological replicates from three different plants. Then the mean values and standard deviations (SD) of the readouts of all of the patches observed for one sample were calculated. All tests of significance between pair treatments were conducted with Duncan's multiple-comparison tests ($P < 0.05$). Different letters mean significant difference between treatments ($P < 0.05$).

Statistical analyses

Microsoft Excel (2016) was used to calculate *P*-values using paired two-tailed Student *t* -test method. The software SPSS version 16.0 (IBM, Chicago, IL, USA) was used for multiple comparisons. Comparisons of sample means were made by one-way analysis of variance (ANOVA, $P < 0.05$) followed by Duncan's multiple comparisons tests, as shown in legends of tables and figures. Detailed statistical analysis data are shown in Supplemental Data Set S13.

Accession numbers

Maize genes analyzed in this study were identified in MaizeGDB (https://www.maizegdb.org/) under the following accession numbers: *Pbf1*, Zm00001d005100; *O2*, Zm00001d018971; *50-kD γ-zein*, Zm00001d020591; *27-kD γ-zein*, Zm00001d020592; *18-kD δ-zein*, Zm00001d037436; *Z1D-4*, Zm00001d030855; *Z1B-5*, Zm00001d019155; *Z1C-10*, Zm00001d048812;

Z1C-11, Zm00001d048813; *PPDK2*, Zm00001d010321; *PPDK1*, Zm00001d038163; *AGPL2*, Zm00001d039131; *Adh1*, Zm00001d033931; *GBSSIIa*, Zm0001d019479; *SSIIc*, Zm00001d014150; *Su1*, Zm00001d049753; *Pho1*, Zm00001d034074; *Bt1*, Zm00001d015746; *Sbe1*, Zm00001d014844; *Sbe2a*, Zm0001d003817; *Sbe2b*, Zm00001d016684; *Su4*, *Zm00001d038121*; *ZmWCR1*, Zm00001d042328; *ZmDOF36*, Zm00001d029512; *ZmDOF27*, Zm00001d034651; *ZmDOF33*, Zm00001d012963; Zm*bZIP22*, Zm00001d021191; Zm*bZIP46*, Zm00001d006157; *ZmNKD2*, Zm00001d026113; *ZmNAC130*, Zm00001d008403; *ZmNAC87*, Zm00001d008403; and *ZmbZIP34*, Zm00001d038189. RNA-seq and ChIP-seq data are available from the National Center for Biotechnology Information Gene Expression Omnibus (http://www.ncbi.nlm.nih.gov/geo) under the series entries PRJNA602742 and PRJNA837716, respectively.

Supplemental data

The following materials are available in the online version of this article.

Supplemental Figure S1. The expression of genes related to nitrogen and carbon metabolism in the 6 DAP, 15 DAP, and 24 DAP B73 endosperm under SN and DN conditions.

Supplemental Figure S2. Metabolism overview based on the transcriptome profile of developing B73 endosperm.

Supplemental Figure S3. Regions of motifs associated with DEGs involved in C and N synthesis and metabolism.

Supplemental Figure S4. The phenotypes of *pbf1* mature kernels.

Supplemental Figure S5. Storage-reserve contents of WT and *pbf1* endosperms.

Supplemental Figure S6. Comparison of DEGs detected in our study versus the DEGs between the *pbf1*RNAi and WT generated by Zhang et al. (2016).

Supplemental Figure S7. The expression of 27-kD *γ-zein* in the WT and *pbf1* endosperm under SN and DN conditions.

Supplemental Figure S8. PBF1 protein levels as measured by immunoblot assay in endosperm that grown under SN and DN conditions.

Supplemental Figure S9. Determination of the anti-PBF1 antibody in input samples, post-bind input samples, and elution samples of the ChIP experiment by immunoblot analyses.

Supplemental Figure S10. Frequency distributions of peaks per 100-bp bin corresponding to the distance of peaks to TSSs ranging from −2 kb to + 2 kb.

Supplemental Figure S11. Visualization of ChIP-seq reads and peaks of SN- and DN-binding sites for four gene loci using the Integrated Genome Viewer.

Supplemental Figure S12. EMSA analysis of the complex formation between PBF1 and different binding-probes, respectively.

Supplemental Figure S13. ChIP-qPCR assays confirming the in vivo binding activity of PBF1 to the promoter region of downstream target.

Supplemental Figure S14. ChIP-qPCR assays confirming in vivo binding activity of PBF1 to the promoter region of nonzein targets.

Supplemental Figure S15. Venn diagram showing the overlap of all DEGs regulated by PBF1 and N levels and the targets bound by PBF1 in SN endosperm and DN endosperm, respectively.

Supplemental Figure S16. The expression of *PPDKs* and *27-kD γ-zein* in the B73 endosperm at the developing stage under SN and DN conditions.

Supplemental Figure S17. The positions of the ChIP-qPCR primers in promoters of zein targets.

Supplemental Figure S18. PBF1 as a transcriptional activator.

Supplemental Figure S19. The cooperation of PBF1 with ZmbZIP46 to regulate target expression.

Supplemental Table S1. Zein gene position annotation.

Supplemental Table S2. The expression pattern of zein genes as determined by RNA-seq.

Supplemental Table S3. Results of MEME analysis of the promoter sequences of DEGs related to nitrogen and carbon metabolism.

Supplemental Table S4. Results of MEME-ChIP analysis of the 400-bp sequences flanking the summits of peaks associated with the putative PBF1 bound target genes under SN and DN conditions.

Supplemental Table S5. The position of the EMSA probes/ChIP-qPCR primer used in this study.

Supplemental Table S6. The PBF1-binding patterns of zein subfamily genes in SN endosperm and DN endosperm.

Supplemental Data Set S1. Significantly differentially expression genes (DEGs) from RNA-Seq data in B73 endosperm under SN and DN conditions.

Supplemental Data Set S2. The enriched GOs and KEGGs terms related to nitrogen and carbon synthesis and metabolism.

Supplemental Data Set S3. The clusters of DEGs from MapMan analysis.

Supplemental Data Set S4. The DEGs related to nitrogen and carbon synthesis and metabolism used for motif enrichment analysis.

Supplemental Data Set S5. The DEGs of *pbf1* compared to WT in this study.

Supplemental Data Set S6. Enrichment analysis of the DEGs in *pbf1* endosperm compared with WT endosperm.

Supplemental Data Set S7. The altered expression of PBF1-regulated genes between SN endosperm and DN endosperm.

Supplemental Data Set S8. Associated peaks and functional annotation of PBF1-bound targets in SN endosperm and DN endosperm.

Supplemental Data Set S9. PBF1 directly regulated genes in SN endosperm and DN endosperm, respectively.

Supplemental Data Set S10. GO classifications of PBF1 directly regulated genes with functional annotations in SN endosperm.

Supplemental Data Set S11. The targets bound by PBF1 or/and O2.

Supplemental Data Set S12. Primers used in this study.

Supplemental Data Set S13. Summary of statistical analysis.

Acknowledgments

We thank Prof. Ning Jiang at Michigan State University for critical revision of the manuscript.

The work was financially supported by the Major Independent Research Project of Jiangsu Provincial Key Laboratory of Agrobology (JKLA2021-ZD03), the National Natural Science Foundation of China (32001564), and Jiangsu Agriculture Science and Technology Innovation Fund [CX (21)1003].

Conflict of interest statement. The authors declare no conflicts of interest.

References

Bailey TL, Johnson J, Grant CE, Noble WS (2015) The MEME suite. Nucleic Acids Res **43**(Web Server issue): W39–W49

Bailey TL, Bodén M, Buske FA, Frith M, Grant CE, Clementi L, Ren JY, Li WW, Noble WS (2009) MEME SUITE: tools for motif discovery and searching. Nucleic Acids Res **37**: 202–208

Becraft PW, Gutierrez-Marcos J (2012) Endosperm development: dynamic processes and cellular innovations underlying sibling altruism. Wiley Interdiscip Rev Dev Biol **1**: 579–593

Bernard L, Ciceri P, Viotti A (1994) Molecular analysis of wild-type and mutant alleles at the Opaque-2 regulatory locus of maize reveals different mutations and types of O2 products. Plant Mol Biol **24**: 949–959

Borrás L, Zinselmeier C, Senior ML, Westgate ME, Muszynski MG (2009) Characterization of grain-filling patterns in diverse maize germplasm. Crop Sci **49**: 999–1009

Cazetta JO, Seebaure JR, Below FE (1999) Sucrose and nitrogen supplies regulate growth of maize kernels. Ann Bot **84**: 747–754

Chastain CJ, Heck JW, Colquhoum TA, Voge DG, Gu XY (2006) Post translational regulation of pyruvate orthophosphate dikinase in developing rice (Oryzasativa) seeds. Planta **224**: 924–934

Chen J, Yi Q, Cao Y, Wei B, Zheng LJ, Xiao QL, Xie Y, Gu Y, Li YP, Huang HH, et al. (2015) ZmbZIP91 regulates expression of starch synthesis-related genes by binding to ACTCAT elements in their promoters. J Exp Bot **67**: 1327–1338

Chen J, Zeng B, Zhang M, Wang G, Andrew H, Lai J (2014) Dynamic transcriptome landscape of maize embryo and endosperm development. Plant Physiol **166**: 252–264

Coen ES, Romero JM, Doyle S, Elliott R, Murphy G, Carpenter R (1990) Floricaula: a homeotic gene required for flower development in Antirrhinummajus. Cell **63**: 1311–1322

Crawford NM, Forde BG (2002) Molecular and developmental biology of inorganic nitrogen nutrition. Arabidopsis Book **1**: e0011

De Sena Brandine G, Smith AD (2019) Falco: high-speed FastQC emulation for quality control of sequencing data. F1000Res **8**: 1874

Deng M, Li D, Luo J, Xiao Y, Liu H, Pan Q, Zhang X, Jin M, Zhao M, Yan J (2017) The genetic architecture of amino acids dissection by association and linkage analysis in maize. Plant Biotechnol J **15**: 1250–1263

Deng Y, Wang J, Zhang Z, Wu Y (2020) Transactivation of Sus1 and Sus2 by Opaque2 is an essential supplement to sucrose synthase-mediated endosperm filling in maize. Plant Biotechnol J **18**: 1897–1907

Du HY, Ning LH, He B, Wang YC, Ge M, Xu JY, Zhao H (2020) Cross-species root transcriptional network analysis highlights conserved modules in response to nitrate between maize and sorghum. Int J Mol Sci **21**: 1445

Du L, Xu F, Fang J, Gao S, Tang J, Fang S, Wang H, Tong H, Zhang F, Chu J, et al. (2018) Endosperm sugar accumulation caused by mutation of PHS8/ISA1 leads to pre-harvest sprouting in rice. Plant J **95**: 545–556

Feng F, Qi W, Lv Y, Yan S, Xu L, Yang W, Yuan Y, Chen Y, Zhao H, Song R (2018) Opaque11 is a central hub of the regulatory network for maize endosperm development and nutrient metabolism. Plant Cell **30**: 375–396

Gontarek BC, Neelakandan AK, Wu H, Becraft PW (2016) NKD transcription factors are central regulators of maize endosperm development. Plant Cell **28**: 2916–2936

Guo X, Yuan L, Chen H, Sato SJ, Clemente TE, Holding DR (2013) Nonredundant function of zeins and their correct stoichiometric ratio drive protein body formation in maize endosperm. Plant Physiol **162**: 1359–1369

Gupta S, Malviya N, Kushwaha H, Nasim J, Bisht NC, Singh VK, Yadav D (2015) Insights into structural and functional diversity of Dof (DNA binding with one finger) transcription factor. Planta **241**: 549–562

Gutiérrez RA (2012) Systems biology for enhanced plant nitrogen nutrition. Science **336**: 1673

He W, Liu X, Lin L, Xu A, Hao D, Wei C (2020) The defective effect of starch branching enzyme IIb from weak to strong induces the formation of biphasic starch granules in amylose-extender maize endosperm. Plant Mol Biol **103**: 355–371

Hennen-Bierwagen TA, Liu F, Marsh RS, Kim S, Gan Q, Tetlow IJ, Emes M, James MG, Myers AM (2008) Starch biosynthetic enzymes from developing maize endosperm associate in multisubunit complexes. Plant Physiol **146**: 1892–1908

Holding DR, Larkins BA (2009) Zein storage proteins. *In* BA Larkins, AL Kriz, eds, Molecular Genetic Approaches to Maize Improvement. Springer, Berlin, pp 269–286

Huang L, Tan H, Zhang C, Li Q, Liu Q (2021) Starch biosynthesis in cereal endosperms: An updated review over the last decade. Plant Commun **2**: 100237

Jiang L, Ball G, Hodgman C, Coules A, Zhao H, Lu C (2018) Analysis of gene regulatory networks of maize in response to nitrogen. Genes (Basel) **9**: 151

Jiao Y, Peluso P, Shi J, Liang T, Stitzer MC, Wang B, Campbell MS, Stein JC, Wei X, Chin CS, et al. (2017) Improved maize reference genome with single-molecule technologies. Nature **546**: 524–527

Jung JH, Domijan M, Klose C, Biswas S, Ezer D, Gao M, Khattak E, Box MS, Charoensawan V, Cortijo S, et al. (2016) Phytochromes function as thermosensors in Arabidopsis. Science **354**: 886–889

Kirchberger S, Leroch M, Huynen MA, Wahl M, Neuhaus HE, Tjaden J (2007) Molecular and biochemical analysis of the plastidic ADP-glucose transporter (ZmBT1) from Zea mays. J Biol Chem **282**: 22481–22491

Komar DN, Mouriz A, Jarillo JA (2016) Chromatin immunoprecipitation assay for the identification of Arabidopsis protein-DNA interactions *in vivo*. J Vis Exp **14**: e53422

Kubo A, Colleoni C, Dinges JR, Lin Q, Lappe RR, Rivenbark JG, Meyer AJ, Ball SG, James MG, Hennen-Bierwagen TA, et al. (2010) Functions of heteromeric and homomeric isoamylase-type starch-debranching enzymes in developing maize endosperm. Plant Physiol **153**: 956–969

Langmead B, Trapnell C, Pop M, Salzberg SL (2009) Ultrafast and memory-efficient alignment of short DNA sequences to the human genome. Genome Biol **10**: R25

Lappe RR, Baier JW, Boehlein SK, Huffman R, Lin QH, Wattebled F, Stettes AM, Hannah C, Borisjuk L, Rolletschek H, et al. (2017) Functions of maize genes encoding pyruvate phosphate dikinase in developing endosperm. Proc Natl Acad Sci USA **115**: E24–E33

Leroux BM, Goodyke AJ, Schumacher KI, Abbott CP, Clore AM, Yadegari R, Larkins BA, Dannenhoffer JM (2014) Maize early endosperm growth and development: from fertilization through cell type differentiation. Am J Bot **101**: 1259–1274

Li C, Song RT (2020)The regulation of zein biosynthesis in maize endosperm. Theor Appl Genet **133**: 1443–1453

Li CB, Qiao Z, Qi WW, Wang Q, Yuan Y, Yang X, Tang Y, Mei B, Lv Y, Zhao H, et al. (2015) Genome-wide characterization of cis-acting DNA targets reveals the transcriptional regulatory framework of opaque 2 in maize. Plant Cell **27**: 532–545

Li CB, Yue YH, Chen HJ, Qi WW, Song RT (2018) The ZmbZIP22 transcription factor regulates 27-kD γ-Zein gene transcription during maize endosperm development. Plant Cell **30**: 2402–2424

Li QZ, Li CW, Yang TW (2014) Stress response and memory mediated by DNA methylation in plants. Plant Physiol J **50**: 725–734. In Chinese

Liao CS, Peng YF, Ma W, Liu R, Li CJ, Li XX (2012) Proteomic analysis revealed nitrogen-mediated metabolic, developmental, and hormonal regulation of maize (Zea mays L.) ear growth. J Exp Bot **63**: 5275–5288

Liu F, Makhmoudova A, Lee EA, Wait R, Emes MJ, Tetlow IJ (2009) The amylose extender mutant of maize conditions novel protein-protein interactions between starch biosynthetic enzymes in amyloplasts. J Exp Bot **60**: 4423–4440

Liu H, Shi J, Sun C, Gong H, Fan X, Qiu F, Huang X, Feng Q, Zheng X, Yuan N, et al. (2016) Gene duplication confers enhanced expression of 27-kDa gamma-zein for endosperm modification in quality protein maize. Proc Natl Acad Sci USA **113**: 4964–4969

Lu GY, Wu XM, Chen BY, Gao GZ, Xu K (2007) Evaluation of genetic and epigenetic modification in rapeseed (*Brassica napus*) induced by salt stress. J Integr Plant Biol **49**: 1599–1607

Machanick P, Bailey TL (2011) MEME-ChIP: motif analysis of large DNA datasets. Bioinformatics **27**: 1696–1697

Maitz M, Santandrea G, Zhang ZY, Lal S, Hannah L, Salamini F, Thompson R (2001) rgf1, a mutation reducing grain filling in maize through effects on basal endosperm and pedicel development. Plant J **23**: 29–42

Marzábal P, Gas E, Fontanet P, Vicente-Carbajosa J, Torrent M, Ludevid MD (2008) The maize Dof protein PBF activates transcription of γ-zein during maize seed development. Plant Mol Biol **67**: 441–454

Méchin V, Thévenot C, Le Guilloux M, Prioul JL, Damerval C (2007) Developmental analysis of maize endosperm proteome suggests a pivotal role for pyruvate orthophosphate dikinase. Plant Physiol **43**: 1203–1219

Murray MG, Thompson WF (1980) Rapid isolation of high molecular weight plant DNA. Nucleic Acids Res **8**: 4321–4326

Pan XY, Hasan MM, Li Y, Liao CS, Zheng HY, Liu RY, Li XX (2015) Asymmetric transcriptomic signatures between the cob and florets in the maize ear under optimal- and low-nitrogen conditions at silking, and functional characterization of amino acid transporters ZmAAP4 and ZmVAAT3. J Exp Bot **66**: 6149–6166

Peng H, Zhang J (2009) Plant genomic DNA methylation in response to stresses: potential applications and challenges in plant breeding. Prog Nat Sci **9**: 1037–1045

Prioul JL, Méchin V, Damerval C (2008) Molecular and biochemical mechanisms in maize endosperm development: the role of pyruvate-Pi-dikinase and Opaque-2 in the control of C/N ratio. C R Biol **31**: 772–779

Qi X, Li SX, Zhao Q, Zhu DY, Yu JJ (2017) ZmDof3, a maize endosperm-specific Dof protein gene, regulates starch accumulation and aleurone development in maize endosperm. Plant Mol Biol **93**: 7–20

Robinson MD, McCarthy DJ, Smyth GK (2010) edgeR: a bioconductor package for differential expression analysis of digital gene expression data. Bioinformatics **26**: 139–40

Rueda-Lopez M, Crespillo R, Canovas FM, Avila C (2008) Differential regulation of two glutamine synthetase genes by a single Dof transcription factor. Plant J **56**: 73–85

Saleh A, Alvarez-Venegas R, Avramova Z (2008) An efficient chromatin immunoprecipitation (ChIP) protocol for studying histone modifications in Arabidopsis plants. Nat Protoc **3**: 1018–1025

Schurch NJ, Schofield P, Gierlinski M, Cole C, Sherstnev A, Singh V, Wrobel N, Gharbi K, Simpson GG, Owen-Hughes T, et al. (2016) How many biological replicates are needed in an RNA-seq experiment and which differential expression tool should you use? RNA **22**: 839–851

Seebauer JR, Singletary GW, Krumpelman PM, Ruffo ML, Below FE (2010) Relationship of source and sink in determining kernel composition of maize. J Exp Bot **61**: 511–519

Seung D, Smith AM (2018) Starch granule initiation and morphogenesis–progress in Arabidopsis and cereals. J Exp Bot **70**: 771–784

Singletary GW, Below F (1989) Growth and composition of maize kernels cultured in vitro with varying supplies of carbon and nitrogen. Plant Physiol **89**: 341–346

Singletary GW, Doehlert DC, Wilson CM, Muhitch MJ, Below FE (1990) Response of enzymes and storage proteins of maize endosperm to nitrogen supply. Plant Physiol **94**: 858–864

Subasinghe RM, Liu F, Polack UC, Lee EA, Emes MJ, Tetlow IJ (2014) Multimeric states of starch phosphorylase determine protein–protein interactions with starch biosynthetic enzymes in amyloplasts. Plant Physiol Bioch **83**: 168–179

Sweetlove LJ, Beard KFM, Nunes-Nesi A, Fernie AR, Ratcliffe RG (2010) Not just a circle: flux modes in the plant TCA cycle. Trends Plant Sci **15**: 462–470

Tian T, Liu Y, Yan H, You Q, Yi X, Du Z, Xu W, Su Z (2017) agriGO v2.0: a GO analysis toolkit for the agricultural community. Nucleic Acids Res **45**: 122–129

Triboi E, Martre P, Girousse C, Ravel C, Triboi-Blondel AM (2006) Unraveling environmental and genetic relationships between grain yield and nitrogen concentration for wheat. Eur J Agron **25**: 108–118

Tsai CY, Huber DM, Warren HL (1978) Relationship of the kernel sink for N to maize productivity. Crop Sci **18**: 399–404

Uku R, Liis K, Ivan K, Tambet A, Priit A, Hedi P, Jaak V (2019) g: Profiler: a web server for functional enrichment analysis and conversions of gene lists. Nucleic Acids Res **47**: 191–198

Uribelarrea M, Below FE, Moose SP (2004) Grain composition and productivity of maize hybrids derived from the Illinois protein strains in response to variable nitrogen supply. Crop Sci **44**: 1593–1600

Usadel B, Nagel A, Thimm O, Redestig H, Blaesing OE, Palacios-Rojas N, Selbig J, Hannemann J, Piques MC, Steinhauser D, et al. (2005) Extension of the visualization tool MapMan to allow statistical analysis of arrays, display of corresponding genes, and comparison with known responses. Plant Physiol **138**: 1195–1204

Vicente-Carbajosa J, Moose SP, Parsons RL, Schmidt RJ (1997) A maize zinc-finger protein binds the prolamin box in zein gene promoters and interacts with the basic leucine zipper transcriptional activator Opaque2. Proc Natl Acad Sci USA **94**: 7685–7690

Wallace JC, Lopes MA, Paiva E, Larkins BA (1990) New methods for extraction and quantitation of zeins reveal a high content of gamma-zein in modified opaque-2 maize. Plant Physiol **92**: 191–196

Walley JW, Sartor RC, Shen Z, Schmitz RJ, Wu KJ, Urich MA, Nery JR, Smith LG, Schnable JC, Ecker JR, et al. (2016) Integration of OMIC networks in a developmental atlas of maize. Science **353**: 814–818

Wang JC, Xu H, Zhu Y, Liu QQ, Cai XL (2013) OsbZIP58, a basic leucine zipper transcription factor, regulates starch biosynthesis in rice endosperm. J Exp Bot **64**: 3453–3466

Wang Z, Ueda T, Messing J (1998) Messing Characterization of the maize prolamin box-binding factor-1(PBF-1) and its role in the

developmental regulation of the zein multigene family. Gene **223**: 321–332

Wu B, Yun P, Zhou H, Xia D, Gu Y, Li P, Yao J, Zhou Z, Chen J, Liu R, et al. (2022) Natural variation in WHITE-CORE RATE 1 regulates redox homeostasis in rice endosperm to affect grain quality. Plant Cell **34**: 1912–1932

Wu JD, Chen L, Chen MC, Zhou W, Dong Q, Jiang HY, Cheng BJ (2019) The DOF-Domain Transcription factor ZmDOF36 positively regulates starch synthesis in transgenic maize. Front Plant Sci **10**: 465

Wu Y, Messing J (2012) Rapid divergence of prolamin gene promoters of maize after gene amplification and dispersal. Genetics **192**: 507–519

Wu Y, Messing J (2014) Proteome balancing of the maize seed for higher nutritional value. Front Plant Sci **5**: 240

Xu JH, Messing J (2008) Organization of the prolamin gene family provides insight into the evolution of the maize genome and gene duplications ingrass species. Proc Natl Acad Sci USA **105**: 14330–14335

Yanagisawa S (2000) Dof1 and Dof2 transcription factors are associated with expression of multiple genes involved in carbon metabolism in maize. Plant J **21**: 281–288

Yanagisawa S, Sheen J (1998) Involvement of maize Dof zinc finger proteins in tissue-specific and light-regulated gene expression. Plant Cell **10**: 75–89

Yang T, Guo L, Ji C, Wang H, Wang J, Zheng X, Xiao Q, Wu Y (2021) The B3 domain-containing transcription factor ZmABI19 coordinates expression of key factors required for maize seed development and grain filling. Plant Cell **33**: 104–128

Zhan J, Dannenhoffer JM, Yadegari R (2017) Endosperm development and cell specialization. *In* BA Larkins, ed, Maize Kernel Development. CAB International, pp. 28–43

Zhan J, Li G, Ryu CH, Ma C, Zhang S, Lloyd A, Hunter BG, Larkins BA, Drews GN, Wang X, et al. (2018) Opaque-2 regulates a complex gene network associated with cell differentiation and storage functions of maize endosperm. Plant Cell **30**: 2425

Zhang X, Mogel KJ, Lor VS, Hirsch CN, Vries BD, Kaeppler HF, Tracy WF, Kaeppler SM (2019a) Maize sugary enhancer1 (se1) is a gene affecting endosperm starch metabolism. Proc Natl Acad Sci USA **116**: 20776–20785

Zhang Y, Liu T, Meyer CA, Eeckhoute J, Johnson D, Bernstern B, Nusbaum C, Myers R, Brown M, Li W, et al. (2008) Model-based analysis of chip-seq (macs). Genome Biol **9**: R137

Zhang Z, Dong J, Ji C, Wu Y, Messing J (2019b) NAC-type transcription factors regulate accumulation of starch and protein in maize seeds. Proc Natl Acad Sci USA **116**: 11223–11228

Zhang Z, Yang J, Wu Y (2015) Transcriptional regulation of Zein gene expression in maize through the additive and synergistic action of opaque2, prolamin-box binding factor, and O2 heterodimerizing proteins. Plant Cell **27**: 1162

Zhang Z, Zheng X, Yang J, Messing J, Wu Y (2016) Maize endosperm-specific transcription factors O2 and PBF network the regulation of protein and starch synthesis. Proc Natl Acad Sci USA **113**: 10842–10847

Zheng X, Li Q, Li C, An D, Xiao Q, Wang W, Wu Y (2019) Intra-kernel reallocation of proteins in maize depends on VP1-mediated scutellum development and nutrient assimilation. Plant Cell **31**: 2613–2635

Zheng ZL (2009) Carbon and nitrogen nutrient balance signaling in plants. Plant Signaling Behav **4**: 584–559